



# RETRACTED: Neuroprotective Effects of Ginsenoside-Rg1 Against Depression-Like Behaviors via Suppressing Glial Activation, Synaptic Deficits, and Neuronal Apoptosis in Rats

Cuiqin Fan<sup>1</sup>, Qiqi Song<sup>1</sup>, Peng Wang<sup>1</sup>, Ye Li<sup>1</sup>, Mu Yang<sup>1</sup> and Shu Yan Yu<sup>1,2\*</sup>

<sup>1</sup> Department of Physiology, Shandong University, School of Basic Medical Sciences, Jinan, China, <sup>2</sup> Shandong Provincial Key Laboratory of Mental Disorders, School of Basic Medical Sciences, Jinan, China

## OPEN ACCESS

### Edited by:

Junji Yodoi,  
Kyoto University, Japan

### Reviewed by:

Sermin Genc,  
Dokuz Eylül University, Turkey  
Katherine R. Martin,  
Walter and Eliza Hall Institute of  
Medical Research, Australia

### \*Correspondence:

Shu Yan Yu  
shuyanyu@sdu.edu.cn

### Specialty section:

This article was submitted to  
Inflammation,  
a section of the journal  
Frontiers in Immunology

**Received:** 25 September 2018

**Accepted:** 26 November 2018

**Published:** 07 December 2018

### Citation:

Fan C, Song Q, Wang P, Li Y, Yang M and Yu SY (2018) Neuroprotective Effects of Ginsenoside-Rg1 Against Depression-Like Behaviors via Suppressing Glial Activation, Synaptic Deficits, and Neuronal Apoptosis in Rats. *Front. Immunol.* 9:2889. doi: 10.3389/fimmu.2018.02889

Depression is considered a neuropsychiatric disease associated with various neuronal changes within specific brain regions. We previously reported that ginsenoside-Rg1, a potential neuroprotective agent extracted from ginseng, significantly alleviated depressive-like disorders induced by chronic stress in rats. However, the mechanisms by which ginsenoside-Rg1 exerts its neuroprotective effects in depression remain largely uncharacterized. In the present study we confirm that ginsenoside-Rg1 significantly prevented the antidepressant-like effects in a rat model of chronic unpredictable mild stress (CUMS) and report on some of the underlying mechanisms associated with this effect. Specifically, we found that chronic pretreatment with ginsenoside-Rg1 prior to stress exposure significantly suppressed inflammatory pathway activity via alleviating the overexpression of proinflammatory cytokines and the activation of microglia and astrocytes. These effects were accompanied with an attenuation of dendritic spine and synaptic deficits as associated with an upregulation of synaptic-related proteins in the ventral medial prefrontal cortex (vmPFC). In addition, ginsenoside-Rg1 inhibited neuronal apoptosis induced by CUMS exposure, increased Bcl-2 expression and decreased cleaved Caspase-3 and Caspase-9 expression within the vmPFC region. Furthermore, ginsenoside-Rg1 could increase the nuclear factor erythroid 2-related factor (Nrf2) expression and inhibit p38 mitogen-activated protein kinase (p-p38 MAPK) and nuclear factor  $\kappa$ B (NF- $\kappa$ B) p65 subunit activation within the vmPFC. Taken together, these results suggest that the neuroprotective effects of ginsenoside-Rg1, which may assume the antidepressant-like effect in this animal model of depression, appears to result from amelioration of a CUMS-dependent neuronal deterioration within the vmPFC. Moreover, they also provide support for the therapeutic potential of ginsenoside-Rg1 in the treatment of stress-related mental disorders.

**Keywords:** glial activation, inflammation, synaptic deficit, apoptosis, depression, ginsenoside-Rg1

## INTRODUCTION

Depression is considered a critical psychiatric disorder associated with neuronal dysfunction in specific brain regions that usually result from stress stimuli (1–3). An important factor in the production of neuronal damage is neuroinflammation, which has been shown to be associated with a number of neurological diseases (4–6). Moreover, inflammation has also been shown to play a critical role in the pathogenesis of depression, although the pathophysiological mechanisms are not fully understood (7). Results from previous studies have indicated that increased levels of pro-inflammatory factors including interleukin-1 (IL-1), interleukin-6 (IL-6), tumor necrosis factor- $\alpha$  (TNF- $\alpha$ ), and reactive oxygen species (ROS) are present in patients with major depressive disorder (MDD) (8, 9). These results suggest that activation of inflammatory pathways may represent a significant component in the pathophysiology of MDD (10, 11). Therefore, a detailed characterization of the molecular mechanisms underlying these inflammatory processes in depression phenotypes can provide promising insights into therapeutic approaches that targeting specific deficits resulting in depression.

Recent evidence has indicated that chronic stress could cause structural and functional neuronal changes within specific brain regions (12, 13), the neuropathological abnormalities which also found presented in major depressive patients (3). Previous work within our laboratory has revealed that rats subjected to chronic unpredictable mild stress (CUMS) show neuronal ultrastructural abnormalities involving dendritic spines and synapse deficits in brain regions associated with depression (14, 15). Dysfunctions in synaptic formation or structure are thought to be related to a variety of neurological and neurodegenerative disorders (16–19). However, whether treatment with neuroprotective agents results in amelioration of these specific neuronal abnormalities and thus underlying the antidepressant-like effects upon behavior have yet to be investigated.

Ginsenoside-Rg1, the major active ingredient extract from the herb *Panax ginseng* C.A. Meyer, has been shown to function as a potential neuroprotective agent in several animal models of neurological diseases, such as Alzheimer's disease (AD) (20, 21), and cognition and memory impairments (22, 23). Recent studies within our laboratory have shown that ginsenoside-Rg1 was able to ameliorate depression-like behaviors as well as prevent the reductions in brain-derived neurotrophic factor (BDNF) protein levels in the prefrontal cortex of rats subjected to chronic stress (24). Recently, the ventral medial prefrontal cortex (vmPFC) has emerged as an important brain region in response to the stress stimuli and thus considered may involve in the pathogenesis of depression (25, 26). Such results suggest that the antidepressant-like effects of ginsenoside-Rg1 may in part, be related to its neuroprotective effects. However, the detailed neuronal mechanisms underlying the neuroprotective effects of ginsenoside-Rg1, and, in specific, its relevance to the antidepressant-like effects via inhibiting inflammatory process activities and neuronal damage in depression remain largely unknown.

Therefore, in the present study, we investigated some of the bases for the neuroprotective activity responsible for mediating the antidepressant effects of ginsenoside-Rg1 treatment in the CUMS-induced animal model of depression. These results will provide new insights into the antidepressant mechanisms of ginsenoside-Rg1, which we hypothesize may involve neuroprotective effects through modulation of inflammatory activation, synaptic deficits and neuronal apoptosis within depression-associated disorder.

## MATERIALS AND METHODS

### Animals

Male Wistar rats weighing 220–240 g were obtained from the Shandong University Experimental Animal Centre. All procedures were approved by the Shandong University Animal Care and Use Committee and were performed in accordance with the National Institutes of Health Guide for the Care and Use of Laboratory Animals (National Research Council, 1996). Rats were housed in groups of four per cage under controlled temperature (22–24°C) and light (12-h light/dark cycle) conditions. Food and water were freely available throughout the study except during particular experimental procedures. Rats were acclimatized to the laboratory conditions for at least one week prior to use in the experiments. All efforts were made to minimize pain and numbers of the animals used in these experiments.

### Drugs and Treatment

Ginsenoside-Rg1 was purchased from the National Institute for the Control of Pharmaceutical and Biological Products (Beijing, China). The purity of ginsenoside-Rg1 for experiments was  $\geq 99\%$ . Ginsenoside-Rg1 was dissolved in physiological saline (NaCl, 0.9%) at a concentration of 10 mg/ml. Dose and route of ginsenoside-Rg1 administration used in the present study were conducted as based on previous studies (15, 24). In all experiments, drugs were administered intraperitoneally (i. p.) in a constant volume 30 min prior to CUMS exposure. These treatments were conducted daily over the 5-week period of the experiment. All rats were administered saline (10 ml/kg) daily for three days prior to the experiment to habituate them to the intraperitoneal injections. Rats were randomly allocated to one of the following four groups with  $N = 18/\text{group}$ : (a) control (non-CUMS), (b) CUMS, (c) ginsenoside-Rg1 pretreatment (40 mg/kg) followed by control, (d) ginsenoside-Rg1 pretreatment (40 mg/kg) followed by CUMS.

### CUMS Procedure

The CUMS procedure was conducted as described previously (27). Briefly, rats in the control (non-CUMS) group were housed in groups of four per cage in separate standard laboratory rooms/conditions to avoid the influence of the stress stimulation. Rats in the remaining three groups were housed individually in a separate room and were exposed to stressors daily for 5 weeks. A variety of stressors were used including 24 h food deprivation followed by 24 h water deprivation, cage shaking (2 h), physical restraint (2 h), 5 min cold swimming (at 4°C), cage

moisture (24 h), foot-shock (0.5 mA, 0.5 s), 45° cage tilt (24 h) and overnight illumination. One of these stressors was applied each day and the sequence was presented in a random order (Figure 1A).

## Behavioral Tests

Behavioral tests were conducted after 5 weeks of CUMS exposure by an observer blind as to the treatment regime. The following sequence of tests was administered.

### Sucrose Preference Test

The sucrose preference test was performed as described previously with minor modifications (27). Briefly, in the adaptation phase, rats were placed individually in cages with two bottles of sucrose solution (1%, w/v) for the first 24 h period followed by one bottle of sucrose solution being replaced with tap water for the second 24 h period. In the test phase, rats were first deprived of water and food for 24 h and then exposed to two bottles for 3 h, one containing 100 ml of 1% sucrose solution and the other 100 ml of tap water. Total consumed volumes of sucrose solution and tap water were measured and the sucrose preference

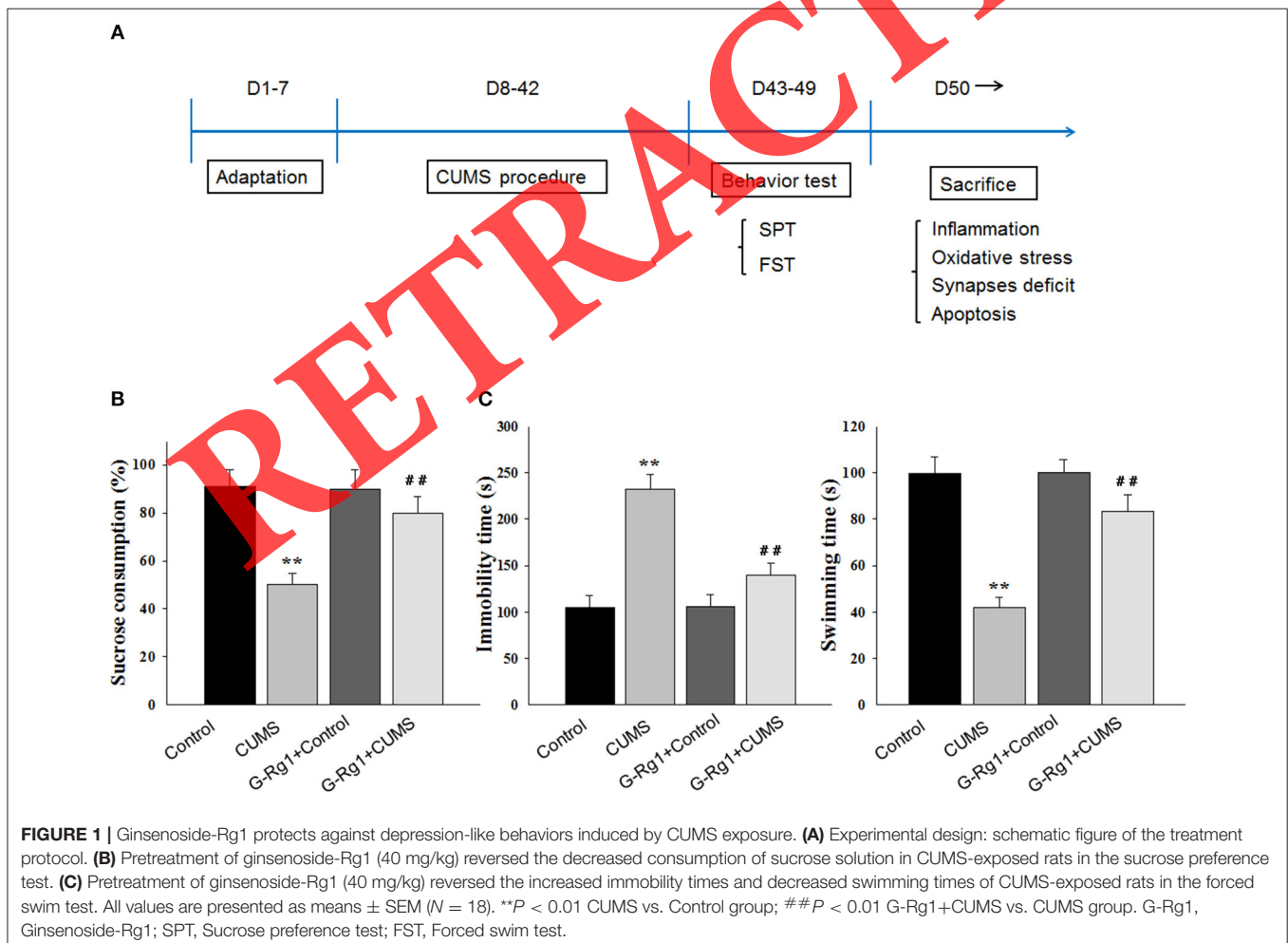
was defined as the sucrose consumption/[water consumption + sucrose consumption] × 100% during the 3 h test.

### Forced Swim Test

Twenty-four hours after the sucrose preference test, rats were subjected to the forced swim test as described previously (28, 29). Briefly, in the initial training phase, rats were placed individually in a cylinder (height: 80 cm, diameter: 30 cm) filled with 50 cm of water at 25 °C for 15 min of forced swimming. Then twenty-four hours later, each rat was placed in the cylinder for a 5-min testing phase. The immobility (floating except for movements required to maintain their head above water) and swimming times were recorded during the swimming test. In this cylinder, rats cannot touch the bottom or escape and the water was changed after each test.

### Brain Dissection

Twenty four hours after behavioral tests, rats were anesthetized with sodium pentobarbital (150 mg/kg, i.p.) and were slowly perfused with 100 mL 0.9% NaCl containing heparin sodium salt followed by 200 mL 4% paraformaldehyde (PFA). After perfusion, the brains were removed and post-fixed with 4%



PFA overnight at 4°C followed by immersions in 10, 20, and 30% sucrose at 4°C for graded dehydration. Parts of brains were then cut into serial coronal frozen sections (30 μm) for immunofluorescence assay, and other brain samples were sliced into 4 μm thick coronal paraffin sections for immunohistochemistry and TUNEL staining. The sections embraced vmPFC regions (coordinates from bregma: +3.24 mm; medial/lateral: ±0.5 mm; dorsal/ventral: −5.0 mm, for Wistar rats at age 8 weeks) were selected for assays.

### Immunofluorescence Assay

The antibodies used for immunofluorescence analysis were primary polyclonal rabbit anti-ionized calcium binding adaptor molecule-1 (Iba-1) (1:500, WAKO, Japan), rabbit anti-gial fibrillary acidic protein (GFAP) (1:100, Proteintech, USA), and goat anti-4-hydroxynonenal (4-HNE, 1:100, ab46545, MA, USA). Primary antibodies were followed by the fluorescent-conjugated secondary antibody (goat anti-rabbit IgG; rabbit anti-goat IgG, 1:200, Sigma-Aldrich). The fluorescent images were acquired using a confocal scanning microscope (LSM780, Carl Zeiss, Germany). At least six representative images were taken from each rat for analysis by Image-Pro plus 6.0 software.

### Immunohistochemistry

Brain sections were deparaffinized and rehydrated as described above. After antigen retrieval, sections were incubated with 3% H<sub>2</sub>O<sub>2</sub> for 10 min and blocked in 5% BSA (containing 0.1% Triton X) for 1 h followed by an overnight incubation at 4°C with primary antibodies to active caspase-3 (1:300), active caspase-9 (1:300), Bcl-2 (1:100), and NeuN (1:400). Following three washes with PBS, the sections were incubated with the horseradish peroxidase (HRP) conjugated goat anti-rabbit IgG (1:200) secondary antibody for 1 h at room temperature. For visualization, sections were stained with 0.05% 3,3'-diaminobenzidine (Sigma). The number of immunoreactive cells in the mPFC area was assessed using light microscopy (Nikon, Japan) at x400 magnification. Ten fields were randomly selected from each section. Cell counts were obtained by averaging the total cell numbers from each animal per group. The positive/total cell numbers were calculated and used to determine active caspase-3, caspase-9, and Bcl-2 expression levels.

### TUNEL Staining

Brain samples were fixed in 4% paraformaldehyde for 24 h and cut into paraffin embedded sections to measure TUNEL positive cells using the In Situ Cell Death Detection Kit<sup>®</sup> (Roche, Germany) following the manufacturer's instructions. Briefly, 4 μm slices were deparaffinized with xylene and rehydrated with graded ethanol concentrations (100, 95, 90, 80, 70%) followed by incubation with protease K (10 μg/ml) at room temperature for 15 min to block non-specific protein interactions. The slices were subsequently incubated with the TUNEL reaction buffer for 1 h at 37°C followed by incubation with 50 μl DAB substrate (DAKO, Denmark) for 10 min at room temperature. The Images were captured with use of light microscopy (Nikon, Japan) at ×400 magnification. At least three different fields (500 × 500 μm) per slice were randomly selected for visualization. The number

of TUNEL positive neurons was counted within 12 randomly selected fields per rat. The positive cell index was expressed as cells/mm and used to indicate apoptosis levels.

## Oxidative Stress Measures

### DHE Analysis

For analysis of brain ROS production, coronal frozen sections (12 μm) of included vmPFC regions were stained with DHE as previously described (30). Briefly, sections were incubated with 10 μM DHE (Invitrogen) for 30 min, and then stained with DAPI (ThermoFisher) for 15 min. Samples were imaged with use of a Zeiss LSM 700 scanning laser confocal microscope. The DHE-staining results were pixelated and quantified using the Image-pro plus image analysis system. Values were expressed relative to the fluorescence signal of respective control images.

### Malondialdehyde (MDA) Concentration

The vmPFC regions were dissected separately and homogenized in ice-cold buffer solution for the determination of MDA content using a commercial assay kit (Nanjing Jiancheng Inc.) with slight modifications as previously described (6). All samples were assayed in duplicate and MDA levels were normalized to the total protein content.

### Western Blot Analysis

Two days after behavioral testing, rats were anesthetized with sodium pentobarbital (150 mg/kg, i.p.), and the dissociated vmPFC tissues homogenate (in 150 mM NaCl, 20 mM Tris-HCl, 2 mM EDTA, 1% Triton X-100, 1 mM PMSF, phosphatase inhibitor cocktail, pH 7.4) was centrifuged at 1000 × g for 15 min at 4°C. The supernatant was collected for biochemical analysis and protein concentration was determined using the BCA protein assay kit (Pierce Bio-technology, Inc., US). Equal amounts of protein from each brain sample (25 μg) were subjected to SDS-PAGE analysis. The resolved proteins were transferred to PVDF membranes (Millipore, Bedford, MA), blocked overnight in 5% nonfat milk, and exposed overnight at 4°C with an appropriate dilution of primary antibodies: anti-BDNF (1:500, Santa Cruz Biotechnology, Santa Cruz, CA), anti-CREB (1:1000), anti-phospho-CREB (1:200) (Cell Signaling Technology, Beverly, MA), anti-PSD-95 (1:800, Santa Cruz Biotechnology, Santa Cruz, CA), anti-synaptophysin (1:1000, Cell Signaling Technology, Beverly, MA), anti-Bcl-2 (1:1000, Cell Signaling Technology, Beverly, MA), anti-Caspase-9 (1:200, Abcam Co., UK), anti-cleaved Caspase-3 (1:500, Abcam Co., UK), anti-p38 MAPK (1:1000), anti-phospho-p38 MAPK (1:500), anti-NF-κB P65 (1:1000), anti-NF-κB phospho-p65 (1:500) (Cell Signaling Technology, Beverly, MA), anti-Nrf2 (1:1000, Abcam Co., UK), and anti-β-actin (1:8000, Santa Cruz Biotechnology, Santa Cruz, CA). The secondary antibody was horseradish peroxidase-conjugated antibody (1:5000, Santa Cruz Biotechnology, Santa Cruz, CA). All proteins were detected using an enhanced chemiluminescence detection kit (GE Healthcare, Buckinghamshire, UK) and protein band densities were quantified by densitometry with β-actin as the loading control using Image-J software (NIH, Scion Corporation,

Frederick, MD). Final data were expressed as a percent of the control. Data were generated from 6 to 8 rats per group.

### Real-Time Quantitative PCR

Total RNA was isolated and extracted from vmPFC samples using the TRIpure Reagent kit (Invitrogen, USA). Total RNA (2  $\mu$ g) was reverse-transcribed into cDNA by using the All-in-One™ miRNA First-Strand cDNA Synthesis Kit (GeneCopoeia, China) according to manufacturer's instructions. The reverse transcription reaction was amplified using a Bio-Rad CFX96 Detection System (Bio-Rad, USA). Quantitative Real time-PCR was performed with use of the ChamQ SYBR qPCR Master Mix (TaKaRa, Japan) on the Bio-rad IQ5 Real Time PCR System (Bio-Rad, USA). Reaction conditions were: 95°C for 30 s and 40 cycles of the amplification step (denaturation at 95°C for 10 s, annealing at 55°C for 10 s and extension at 72°C for 15 s). The specific primers used for qPCR are listed in supplemental data (**Supplementary Table 1**). GAPDH served as a loading control in each sample and gene expression levels of interest were evaluated using the 2<sup>-</sup>( $\Delta\Delta$ Ct) method.

### Enzyme Linked Immunosorbent Assay (ELISA)

Concentrations of IL-1 $\beta$ , IFN- $\gamma$ , and TNF- $\alpha$  were measured with use of an ELISA kit (Abcam Co., UK) according to the manufacturer's instructions. Total protein isolated from vmPFC tissue samples was determined with use of the BCA assay (Thermo Fisher, Waltham, MA). Equal amounts of diluted samples were added to each well of the ELISA kit (96 wells) coated with the appropriate antibody. Data were expressed as the amount of cytokine (pg) per total protein (mg) (mean  $\pm$  SEM). Data were generated from 6 to 8 rats per group.

### Golgi Staining

Golgi staining was performed to document any potential changes in neuronal dendrites and dendritic spines within vmPFC neurons using the FD Rapid GolgiStain™ Kit (FD Neuro-Technologies, MD21041, USA) according to the manufacturer's instructions. Briefly, brains were immersed in the impregnation solution (A/B = 1:1, total 15 ml/rat) at room temperature in the dark. Two weeks later, brains were transferred into Solution C and stored at 4°C in the dark for three days. Brains were then sectioned serially into 100  $\mu$ m coronal sections and each section was transferred to a gelatin-coated slide with solution C and then dried naturally at room temperature in the dark for up to 3 days. The sections were then placed in a mixture consisting of solution D, solution E, and distilled water (1:1:2) for 10 min followed by a dehydration series consisting of 50, 75, 95, and 100% ethanol, for 4 applications at 4 min each. The sections were then cleaned in xylene and cover-slipped with Rhamsan gum for light microscopic observation. In each section, at least 3–5 dendritic segments of apical dendrites per neuron were randomly selected, and 5 pyramidal neurons were analyzed per animal. For each group, at least 4 rats were analyzed with use of Image-Pro plus 6.0 software.

### Transmission Electron Microscopy (TEM)

Transmission electron microscopy (TEM) analysis was performed to assess vmPFC neuronal ultrastructure. The tissues were then placed in 2.5% glutaraldehyde at 4°C for 4 h followed by fixation with 1% osmium tetroxide for 2 h. After a series of graded ethanol dehydrations, the tissues were infiltrated with a mixture of one-half propylene oxide overnight and embedded in resin. The tissues were then cut into ultrathin sections (70 nm) and stained with 4% uranyl acetate for 20 min followed by 0.5% lead citrate for 5 min. Ultrastructure of the vmPFC was then observed with use of TEM (Philips Tecnai 20 U-Twin, Holland). In this study, at least 30 micrographs were randomly taken from each rat for analysis using Image J analysis software (NIH, Scion Corporation, Frederick, MD).

### Statistical Analysis

Data were presented as the mean  $\pm$  standard error of the mean. The results were analyzed with SPSS version 13.0 (SPSS Inc., Chicago, IL, United States). Statistical significance of differences among groups was evaluated by one-way or two-way analysis of variance (ANOVA) with the Tukey's multiple-comparison test for *post-hoc* comparisons.  $P < 0.05$  was required for results to be considered statistically significant.

## RESULTS

### Ginsenoside Rg1 Treatment Ameliorated Depression-Like Behaviors Resulting From CUMS Exposure

Results obtained from the sucrose preference test showed that the percent of sucrose consumption was significantly different among the four groups [ $F_{(3,68)} = 20.65$ ,  $P < 0.01$ ] (**Figure 1B**). *Post-hoc* analysis revealed that 5-weeks of CUMS exposure significantly reduced the percent of sucrose consumption in stressed rats as compared with that of the non-stressed control group ( $P < 0.01$ ), while chronic pretreatment of ginsenoside-Rg1 (40 mg/kg daily) significantly increased the percent of sucrose consumption in CUMS-exposed rats as compared to that of the stressed rats ( $P < 0.01$ ). There were no statistically significant differences between the ginsenoside-Rg1 pretreated control group and control groups with regard to sucrose consumption ( $p > 0.05$ ).

Results of the forced swim test showed that there were significant differences among the four groups with regard to both immobility [ $F_{(3,68)} = 17.32$ ,  $P < 0.01$ ] and swimming [ $F_{(3,68)} = 16.89$ ,  $P < 0.01$ ] times (**Figure 1C**). *Post-hoc* analysis indicated that 5-weeks of CUMS exposure significantly increased immobility times ( $P < 0.00$ ) and decreased swimming times ( $P < 0.01$ ) in rats as compared to the non-stressed control group. In contrast, pretreatment with ginsenoside-Rg1 reversed these effects, with statistically significant decreases in immobility and increases in swim times now being observed in the ginsenoside-Rg1 and CUMS-exposure as compared to the stressed rats ( $P < 0.01$ ). No significant differences in immobility and swim times were obtained between the ginsenoside-Rg1 pretreated control group and control groups in the forced

swim test ( $P > 0.05$ ). Overall, the results obtained from these behavioral tests demonstrate that chronic ginsenoside-Rg1 treatment exerted a potential antidepressant-like effect in this CUMS-induced depression rat model.

### Ginsenoside-Rg1 Treatment Reduced CUMS Exposure-Induced Microglial Activation and Inflammatory Cytokine Expression Within the vmPFC

Activation of glia cells was used as a means to assess possible involvement of neuroinflammatory responses as related to the anti-depressant effects induced by ginsenoside-Rg1. The results of the Iba1 immunohistochemistry assay showed that after 5-weeks of CUMS exposure, vmPFC microglial morphology demonstrated obvious alterations as compared with that of non-stressed rats, characterized by soma enlargement and ramified process retraction (Figure 2A). In addition to these morphological changes, ANOVA revealed that the number of Iba-1<sup>+</sup> microglia within the vmPFC region was significantly different among the four groups [ $F_{(3,20)} = 18.72$ ,  $P < 0.01$ ]. *Post-hoc* analysis indicated that the 5-weeks of CUMS exposure significantly increased the number of activated vmPFC microglia as compared to the non-stressed control rats ( $P < 0.001$ ). These changes in microglia number were significantly reversed by chronic pretreatment with ginsenoside-Rg1 ( $P < 0.01$ ). No significant differences were obtained between the ginsenoside-Rg1 pretreated control group and control groups with regard to the Iba-1<sup>+</sup> microglia number ( $p > 0.05$ ).

Inflammatory responses mediated by activation of glia cells usually trigger cytokine secretions. Therefore, expressions of several critical pro-inflammatory cytokines were measured. Results showed that there were significant differences among the four groups with regard to the mRNA (Figure 2B) and protein (Figure 2C) levels of IL-1 $\beta$  [qPCR:  $F_{(3,20)} = 21.26$ ,  $P < 0.01$ ; ELISA:  $F_{(3,20)} = 18.74$ ;  $P < 0.01$ ], IFN- $\gamma$  [qPCR:  $F_{(3,20)} = 15.92$ ,  $P < 0.01$ ; ELISA:  $F_{(3,20)} = 16.19$ ,  $P < 0.01$ ] and TNF- $\alpha$  [qPCR:  $F_{(3,20)} = 18.33$ ,  $P < 0.01$ ; ELISA:  $F_{(3,20)} = 16.76$ ,  $P < 0.01$ ]. *Post-hoc* analysis indicated that 5-weeks of CUMS exposure significantly increased expression levels of pro-inflammatory cytokines within the vmPFC as compared to that observed in the non-stressed control group ( $P < 0.001$ ). Ginsenoside-Rg1 treatment significantly prevented these increases in cytokines resulting from CUMS as compared with that of the CUMS-exposed groups ( $P < 0.01$ ). There were no differences between the ginsenoside-Rg1 pretreated control group and control groups with regard to IL-1 $\beta$ , IFN- $\gamma$ , and TNF- $\alpha$  expression within the vmPFC ( $p > 0.05$ ).

### Ginsenoside-Rg1 Treatment Decreased CUMS Exposure-Induced Reactive Astroglia Within the vmPFC

As astroglial activation also plays a crucial role in neuroinflammatory responses, we next investigated the effect of ginsenoside-Rg1 on astroglial activation in this depression animal model. As shown in Figure 3A, there were significant differences among the four groups with regard to the number

of GFAP positive astroglia within the vmPFC region [ $F_{(3,20)} = 17.09$ ,  $P < 0.01$ ]. *Post-hoc* analysis indicated that the 5-weeks of CUMS exposure induced a remarkable activation of astroglial responses within the vmPFC of rats ( $P < 0.001$ ), an effect which was significantly prevented by chronic ginsenoside-Rg1 administration ( $P < 0.01$ , Figure 3B). Moreover, astroglial GFAP up regulation, together with the cellular hypertrophy and protuberance extension were also observed in vmPFC regions after CUMS exposure as determined using confocal microscopy ( $p < 0.01$ , Figures 3A,C). In addition, CUMS exposure also reduced GFAP expression as determined with Western Blot [ $F_{(3,20)} = 14.82$ ,  $P < 0.01$ ], while pre-treatment with ginsenoside-Rg1 prevented this effect of chronic stress on astroglial activation ( $P < 0.05$ , Figure 3D). These results indicate that CUMS exposure produces a substantial increase in glial activation within the vmPFC, and that ginsenoside-Rg1 treatment can significantly suppress this effect.

### Ginsenoside-Rg1 Treatment Attenuated CUMS Exposure-Induced Oxidative Stress Within vmPFC Neurons

Results from the DHE assay demonstrated that ROS levels were significantly increased after 5-weeks of CUMS exposure as compared with that of the non-stressed group [ $F_{(3,20)} = 15.79$ ,  $P < 0.01$ ] (Figures 4A,C). Pre-treatment with ginsenoside-Rg1 significantly reduced ROS levels as compared with that obtained within the CUMS exposed groups ( $P < 0.01$ ). 4-HNE, a stable product of lipid peroxidation, has been implicated as a key mediator of oxidative stress induced cell death. Similarly, vmPFC 4-HNE levels were significantly increased in CUMS exposed rats (Figures 4B,D), while ginsenoside-Rg1 pre-treatment displayed evidence of reducing this oxidative stress as indicated by decreased 4-HNE staining relative to that observed in CUMS-exposed rats ( $P < 0.05$ ). These results reveal that early increase in oxidative damage within the vmPFC is one consequence of CUMS exposure. Moreover, increased levels of MDA in response to CUMS exposure were also observed within the vmPFC region, whereas ginsenoside-Rg1 pre-treatment suppressed this generation of CUMS-induced MDA [ $F_{(3,20)} = 16.18$ ,  $P < 0.05$ ] (Figure 4E). Together, these data suggest that ginsenoside-Rg1 exerts protective effects on *in vivo* stress-induced oxidative damage.

### Ginsenoside-Rg1 Treatment Attenuated CUMS Exposure-Induced Changes in Synaptic Structure Within the vmPFC

To determine further whether neuronal deficits induced by CUMS exposure, involve structural changes in vmPFC neurons which can be prevented by neuroprotective mechanisms of ginsenoside-Rg1, a Golgi staining assay was used to assess dendritic spine densities. Results from the Golgi staining assay showed that the density of dendritic spines were significantly different among the four groups [ $F_{(3,12)} = 19.64$ ,  $P < 0.01$ ] (Figure 5A). *Post-hoc* analysis showed that 5-weeks of CUMS exposure markedly decreased the density of dendritic spines

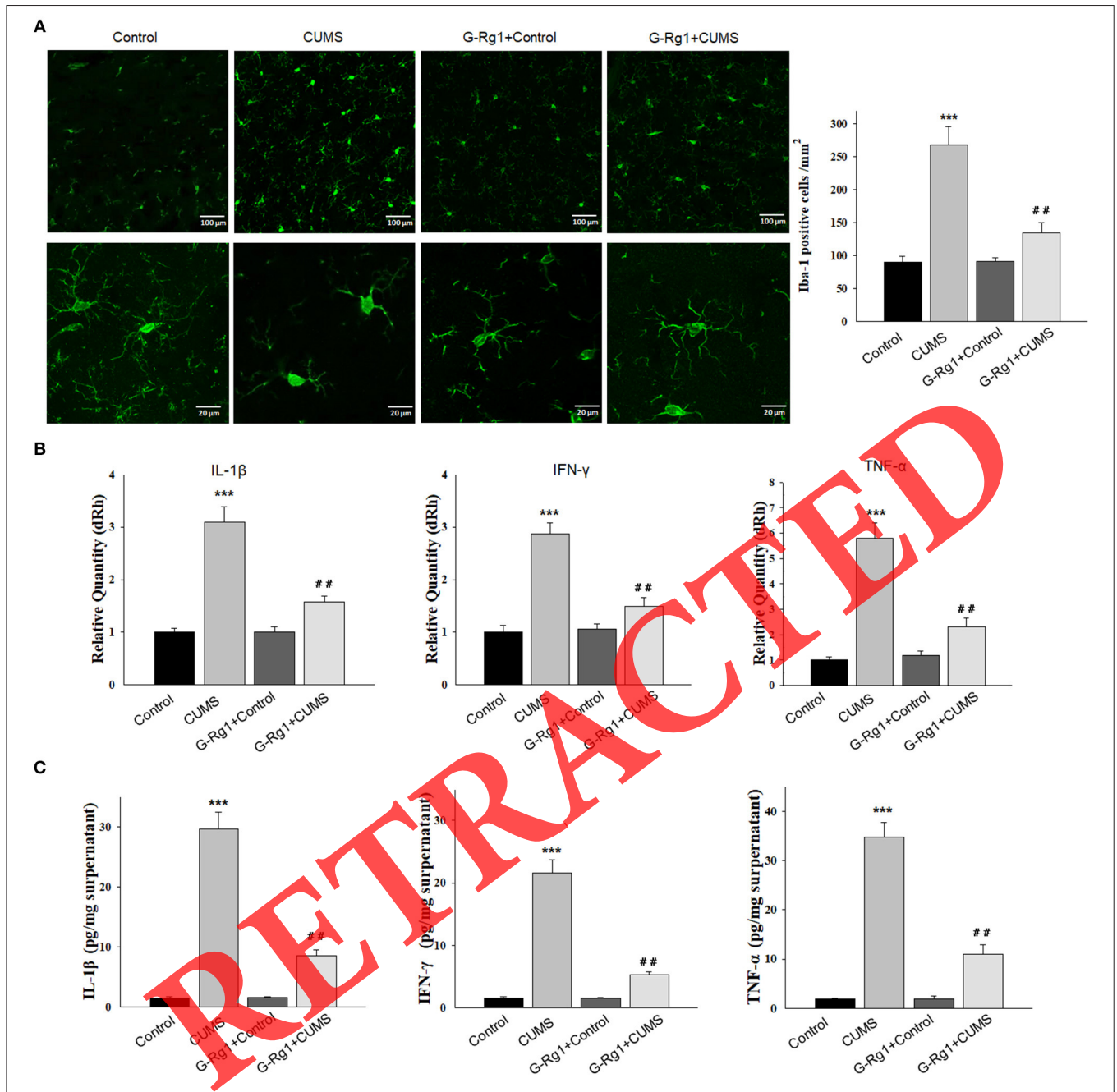


**FIGURE 2 |** Ginsenoside-Rg1 attenuated microglial activation and inflammatory cytokine expressions induced by CUMS-exposure. **(A)** CUMS exposure significantly increased the number of Iba1 positive microglial cells within the vmPFC. Microglial cells retracted their processes and assumed a rounded morphology indicative of activated microglia. All of these CUMS-induced effects were significantly attenuated by ginsenoside-Rg1 pretreatment. **(B)** Real-time quantitative PCR assays showed that CUMS exposure increased IL-1 $\beta$ , IFN- $\gamma$ , and TNF- $\alpha$  mRNA expression within the vmPFC, effects which were suppressed by ginsenoside-Rg1. **(C)** ELISA assays showed that CUMS exposure increased IL-1 $\beta$ , IFN- $\gamma$ , and TNF- $\alpha$  protein expressions within the vmPFC, effects which were ameliorated by ginsenoside-Rg1. Data were presented as the means  $\pm$  SEM ( $N = 6$ ). \*\*\* $P < 0.001$  CUMS vs. Control group; \*\* $P < 0.01$  G-Rg1+CUMS vs. CUMS group. G-Rg1, Ginsenoside-Rg1.

within vmPFC regions as compared with that of the non-stressed control group. These CUMS exposure-induced changes in dendritic spine densities were significantly ameliorated by pretreatment with ginsenoside-Rg1 ( $P < 0.05$ ). We also examined the synaptic ultrastructure of vmPFC neurons using transmission

electron microscopy. ANOVA showed an overall significant difference among the four groups with regard to the synaptic number density within the vmPFC [ $F_{(3,12)} = 17.61, P < 0.01$ ]. As shown in **Figure 5B**, 5-weeks of CUMS exposure resulted in a significant decrease in MPFC synapse numbers as compared

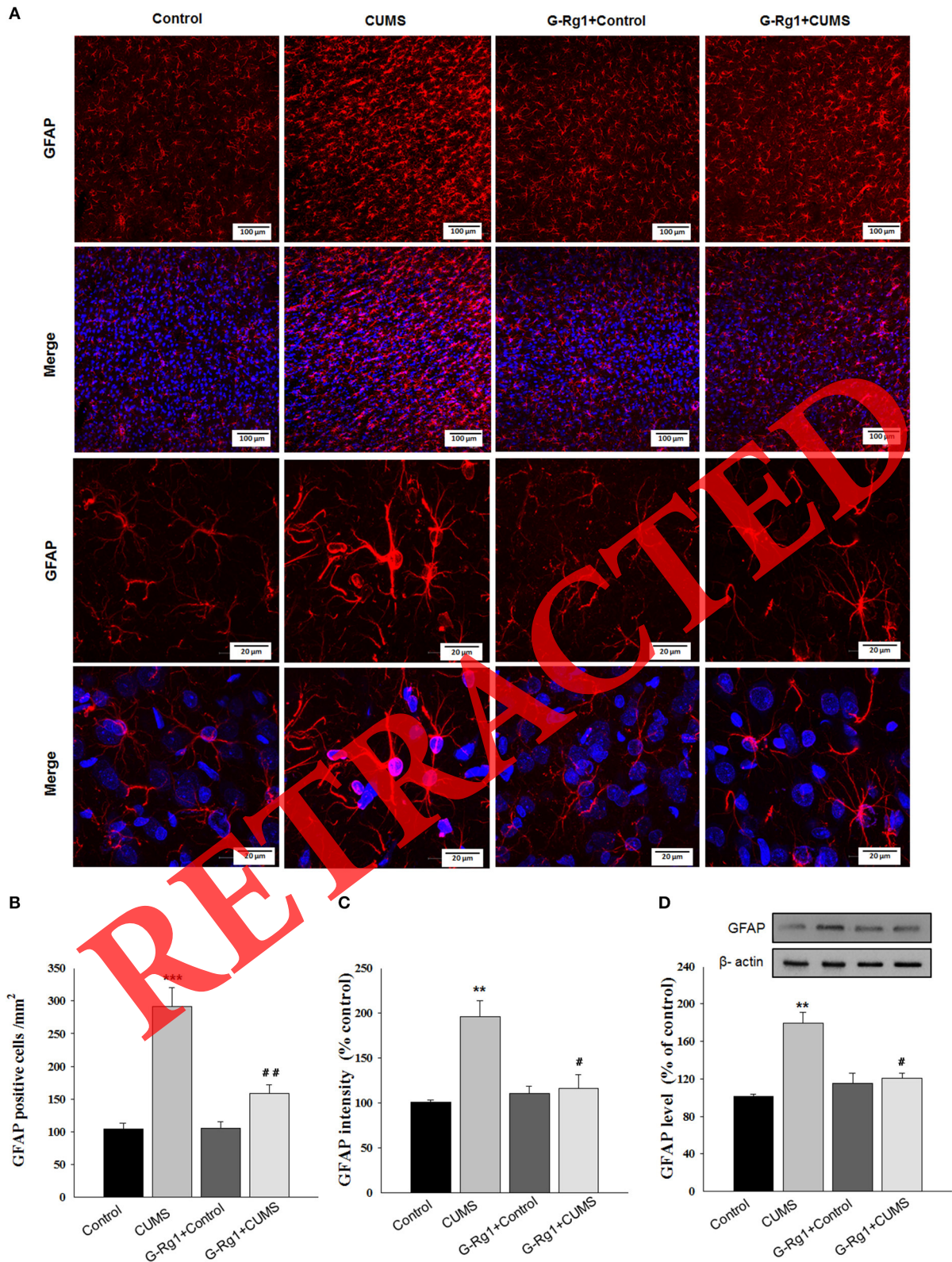


**FIGURE 3 |** Ginsenoside-Rg1 ameliorated reactive astrogliosis within the vmPFC as induced by CUMS-exposure. **(A)** CUMS exposure significantly increased the number of GFAP (red) positive astroglial cells within the vmPFC, effects which were attenuated by ginsenoside-Rg1 pretreatment. Nuclei (blue) are stained with DAPI. *(Continued)*



**FIGURE 3** | Scale bar is 100  $\mu\text{m}$  (upper) or 20  $\mu\text{m}$  (bottom). **(B)** Bar graph illustrating the mean number of astrocytes within the vmPFC region of rats. At least 12 micrographs from 6 rats per group were analyzed. **(C)** Bar graph illustrating the fluorescence intensity of GFAP within the vmPFC region of rats. **(D)** GFAP levels within the vmPFC region were measured at 3 days after CUMS with use of Western blot. Bar graphs show quantification of GFAP levels from Western blot.  $N = 6$  per group. Data were presented as the means  $\pm$  SEM. \*\* $P < 0.01$ , \*\*\* $P < 0.001$  CUMS vs. Control group; # $P < 0.05$ , ## $P < 0.01$  G-Rg1+CUMS vs. CUMS group. (G-Rg1, Ginsenoside-Rg1).

to that of the non-stressed control group, whereas chronic pretreatment with ginsenoside-Rg1 significantly ameliorated this synaptic loss ( $P < 0.05$ ). No significant differences between the ginsenoside-Rg1 pretreated control group and control groups were obtained with regard to dendritic spine and synapse density within the vmPFC ( $P > 0.05$ ). These morphological results indicate that the neuroprotective ability of ginsenoside-Rg1 upon the structure of vmPFC neurons may serve as one of the important mechanistic bases for its antidepressant-like effects.

### Ginsenoside-Rg1 Treatment Up-Regulates Synaptic-Related Protein Expression Within the vmPFC

Whether CUMS-exposure also affects synaptic-associated proteins and the potential modulation of this effect by ginsenoside-Rg1 treatment was investigated through use of assays involving the expression and/or activity of CREB, BDNF, PSD-95, and synaptophysin, all of which are considered to be involved in neuronal synaptogenesis processes. Results from immunofluorescence assays showed that these biochemical markers of immunoreactive cells were all significantly reduced in vmPFC regions after 5-weeks of CUMS-exposure when compared with the non-stressed control group [p-CREB:  $F_{(3,20)} = 16.73$ ,  $P < 0.01$ ; BDNF:  $F_{(3,20)} = 14.96$ ,  $P < 0.01$ ; PSD-95:  $F_{(3,20)} = 17.28$ ,  $P < 0.01$ ; synaptophysin:  $F_{(3,20)} = 15.57$ ,  $P < 0.01$ ] (**Figures 6A,B**). In contrast, ginsenoside-Rg1 treatment significantly up-regulated levels of these immunoreactive cells as compared to the CUMS-exposed group ( $p < 0.05$ ).

The results from western blot assays also showed that there was a significant decrease in the phosphorylation of CREB protein [ $F_{(3,20)} = 15.89$ ,  $P < 0.01$ ], as well as a decrease in the expression of BDNF [ $F_{(3,20)} = 17.15$ ,  $P < 0.01$ ], PSD-95 [ $F_{(3,20)} = 18.76$ ,  $P < 0.01$ ], and synaptophysin [ $F_{(3,20)} = 16.44$ ,  $P < 0.01$ ] in response to CUMS exposure (**Figure 6C**). Chronic pretreatment with ginsenoside-Rg1 significantly ameliorated this CUMS-induced down-regulation of these synaptic-related protein expressions ( $P < 0.05$ ). These findings indicate that the amelioration of CUMS exposure-induced reductions in synaptic-related protein expressions by ginsenoside-Rg1 may represent another significant mechanistic component involved with its antidepressant-like effects to CUMS-exposure.

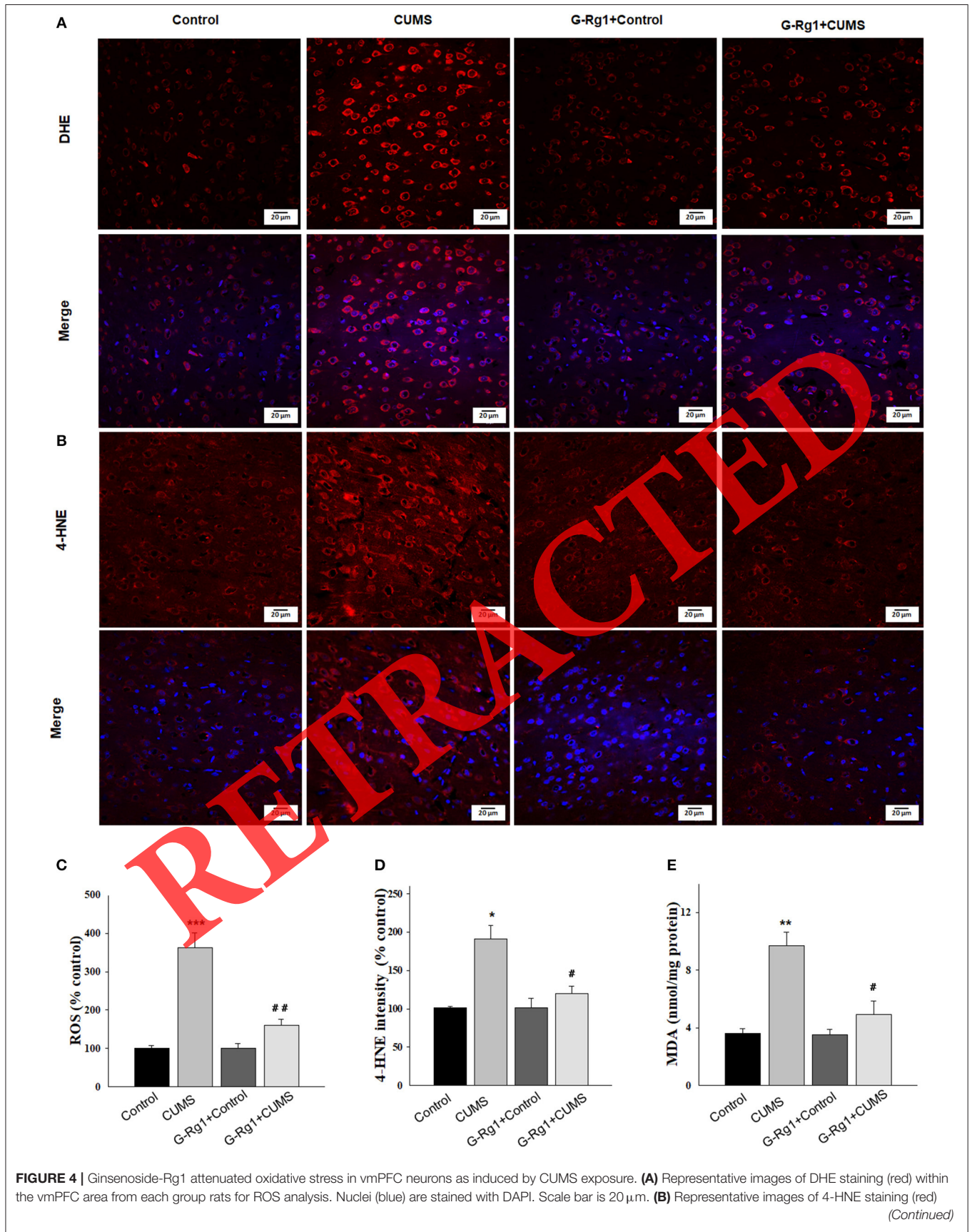
### Ginsenoside-Rg1 Treatment Reduced CUMS Exposure-Induced Neuronal Apoptosis Within the vmPFC

In order to assess the apoptotic effects of CUMS-exposure, the TUNEL Staining assay was initially used to observe the density of apoptotic cells within the vmPFC. As shown in **Figures 7A,E**, TUNEL positive labeled cells displayed an overall statistically

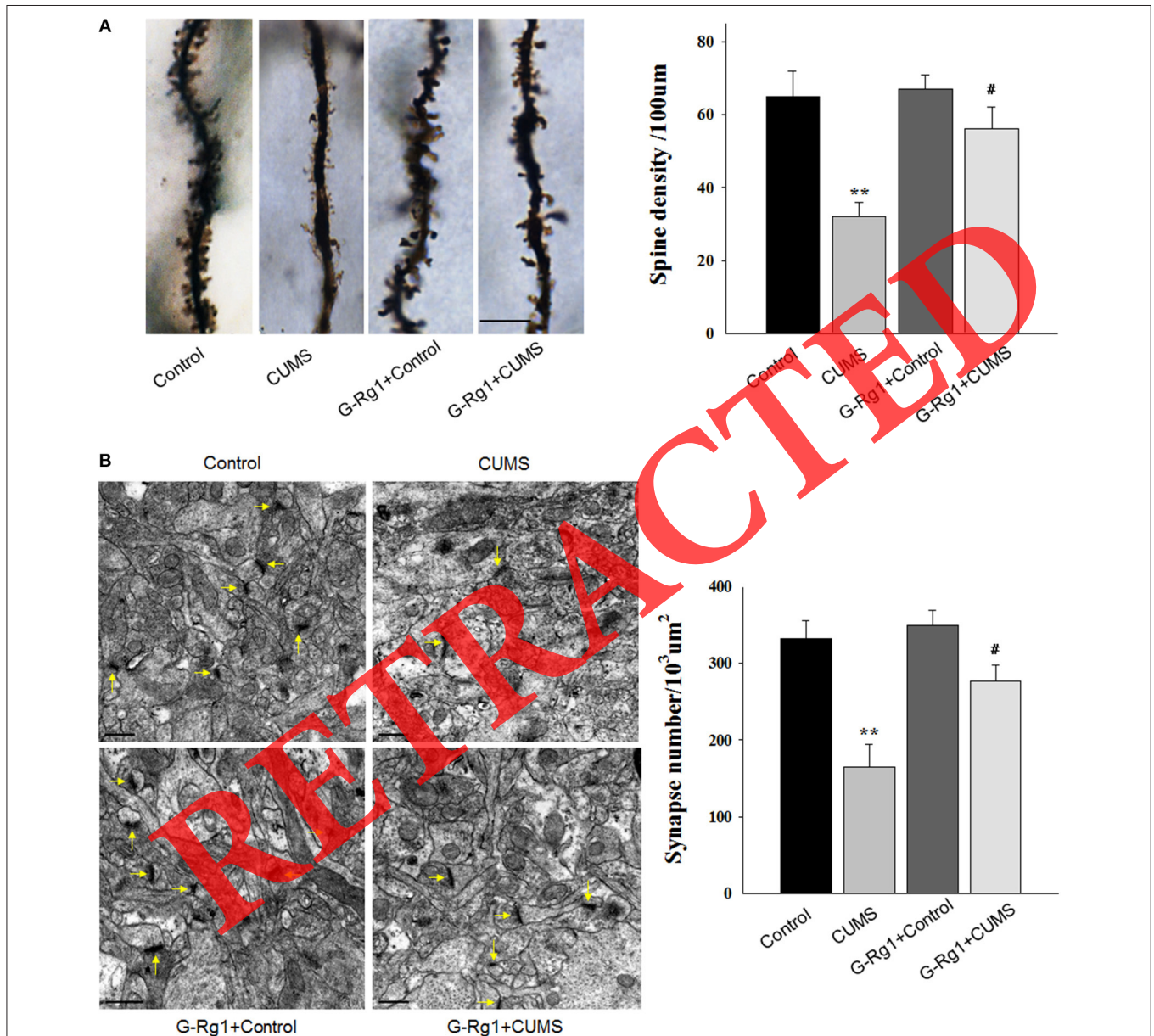
significant difference among the four groups [ $F_{(3,20)} = 17.23$ ,  $P < 0.01$ ]. *Post-hoc* analysis indicated that the density of apoptotic cells significantly increased within the vmPFC of CUMS-exposed rats as compared with that of the non-stressed control group ( $P < 0.001$ ). Moreover, immunohistochemistry assays showed that NeuN positive labeled cells were also significantly decreased within the vmPFC regions after 5-weeks of CUMS-exposure ( $P < 0.01$ ) (**Figures 7B,F**). Chronic ginsenoside-Rg1 pretreatment markedly inhibited this massive cell loss in the vmPFC area of CUMS-exposed rats ( $P < 0.05$ ). Furthermore, NeuN/cleaved Caspase 3 positive double labeled cells were significantly increased within the vmPFC regions after 5-weeks of CUMS-exposure ( $P < 0.01$ ) (**Figures 7C,G**), which could be reversed by chronic ginsenoside-Rg1 pretreatment ( $P < 0.05$ ). TEM results demonstrated that vmPFC neurons within CUMS-exposure rats showed strong staining within condensed portions of chromosomes, which were accompanied with nuclear chromatin margination, aggregation and condensation. In contrast, these apoptotic morphological changes induced by CUMS exposure were obviously alleviated by chronic pretreatment with ginsenoside-Rg1 (**Figure 7D**).

### Ginsenoside-Rg1 Treatment Suppressed CUMS Exposure-Induced Expression of Apoptosis-Related Proteins Within the vmPFC

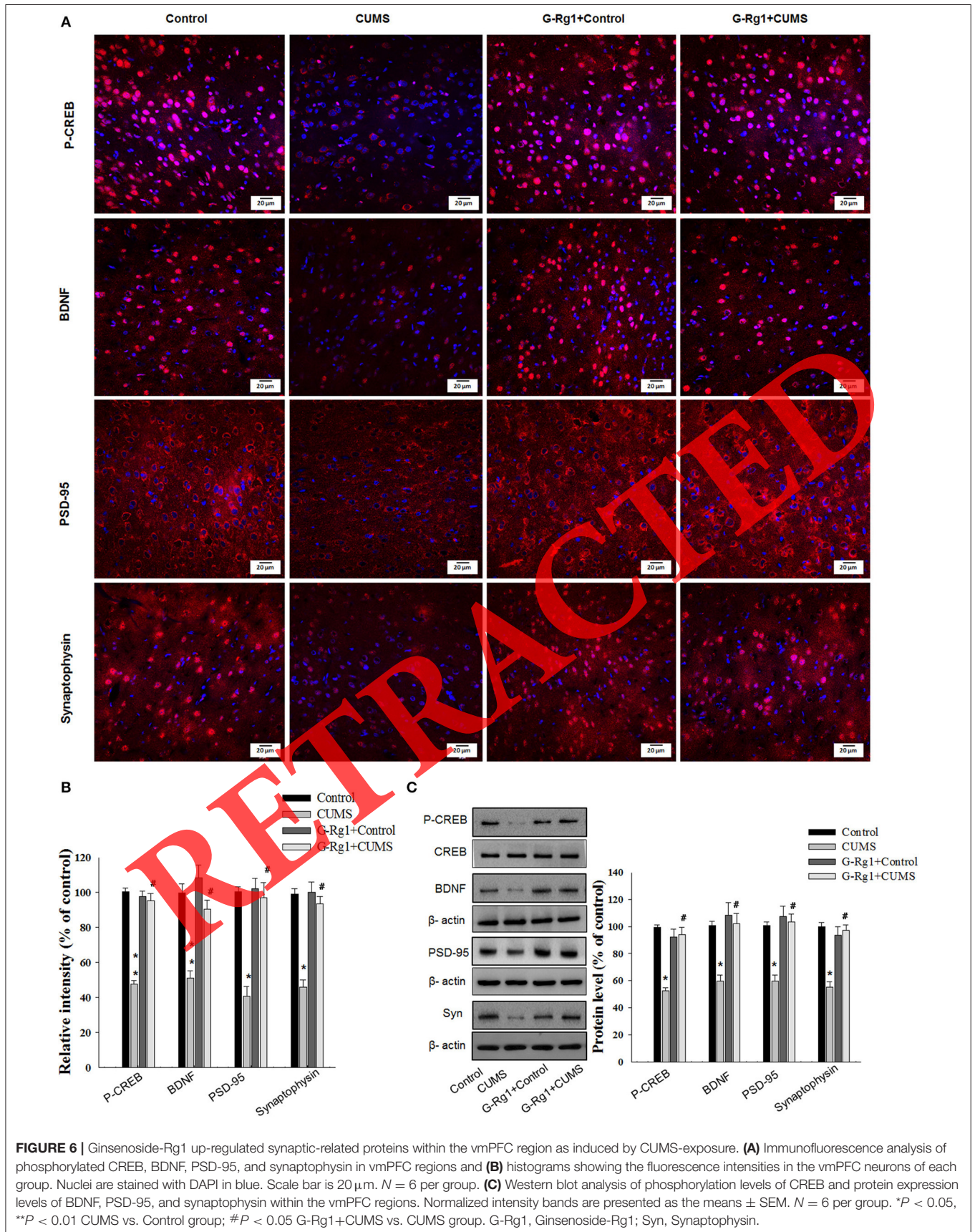
To corroborate the above results, we next examined the effects of CUMS-exposure on the expression of apoptosis-related proteins. Our results revealed that there were significant differences among the four groups with regard to immunoreactive (**Figures 8A,B**) and protein (**Figure 8C**) levels of cleaved caspase-3 [IHC:  $F_{(3,12)} = 16.75$ ,  $P < 0.01$ ; WB:  $F_{(3,20)} = 13.49$ ,  $P < 0.05$ ], caspase-9 [IHC:  $F_{(3,12)} = 15.17$ ,  $P < 0.01$ ; WB:  $F_{(3,20)} = 14.56$ ,  $P < 0.05$ ], and Bcl-2 [IHC:  $F_{(3,12)} = 15.32$ ,  $P < 0.01$ ; WB:  $F_{(3,20)} = 12.29$ ,  $P < 0.05$ ]. *Post-hoc* analysis indicated that ginsenoside-Rg1 pretreatment significantly prevented the increased expression levels of Caspase-3 and Caspase-9, along with the decreased expression levels of Bcl-2 within the vmPFC which resulted from CUMS exposure ( $P < 0.01$ ). Taken together, these results provide evidence that suppression of pro-apoptotic factors expression and neuronal apoptosis may contribute to the antidepressant-like effects of ginsenoside-Rg1. In addition, to clarify the possible mechanisms of the anti-inflammatory and anti-apoptotic effects of ginsenoside-Rg1, our results further revealed that there were significant differences among the four groups with regard to the phosphorylated levels of p38 MAPK [ $F_{(3,20)} = 14.86$ ;  $P < 0.05$ ], NF- $\kappa$ B p65 subunit [ $F_{(3,20)} = 15.73$ ;  $P < 0.05$ ], and protein levels of Nrf2 [ $F_{(3,20)} = 12.94$ ;  $P < 0.05$ ]. *Post-hoc* analysis indicated that ginsenoside-Rg1 pretreatment significantly prevented the



**FIGURE 4** | vmPFC area from each group rats. Nuclei (blue) are stained with DAPI. Scale bar is 20  $\mu\text{m}$ . **(C)** Bar graph illustrating the quantitative data of relative fluorescence of ROS within the vmPFC area of rats. Values are expressed relative to those of the control group.  $N = 6$  per group. **(D)** Bar graph illustrating the quantification of 4-HNE within the vmPFC area of rats. Values are expressed relative to those of the control group.  $N = 6$  per group. **(E)** MDA analysis was performed and levels were normalized to the protein content.  $N = 10$  per group. Data were presented as the means  $\pm$  SEM.  $*P < 0.05$ ,  $**P < 0.01$ ,  $***P < 0.001$  CUMS vs. Control group;  $\#P < 0.05$ ,  $\#\#P < 0.01$  G-Rg1+CUMS vs. CUMS group. G-Rg1, Ginsenoside-Rg1.



**FIGURE 5** | Ginsenoside-Rg1 ameliorated the deficits of dendritic spine and synapse in vmPFC neurons as induced by CUMS exposure. **(A)** Representative images of Golgi staining of the vmPFC area from each group rats. Scale bar is 10  $\mu\text{m}$ . Bar graph illustrating the mean spine density of dendrites within the vmPFC area of rats. At least 12 dendritic segments (100  $\mu\text{m}$ ) from neurons of 4 rats per group were analyzed. **(B)** Representative electron micrograph of vmPFC neurons in rats from each group. Arrows indicate spine synapses. Scale bar is 0.5  $\mu\text{m}$ . Bar graph illustrating the mean synapse density within the vmPFC area. At least 30 micrographs from neurons of 4 rats per group were analyzed. Chronic pretreatment with ginsenoside-Rg1 significantly ameliorated the decrease of vmPFC neuronal dendritic spines and synapses in CUMS-exposed rats. Data were presented as the means  $\pm$  SEM.  $**P < 0.01$  CUMS vs. Control group;  $\#P < 0.05$  G-Rg1+CUMS vs. CUMS group. G-Rg1, Ginsenoside-Rg1.



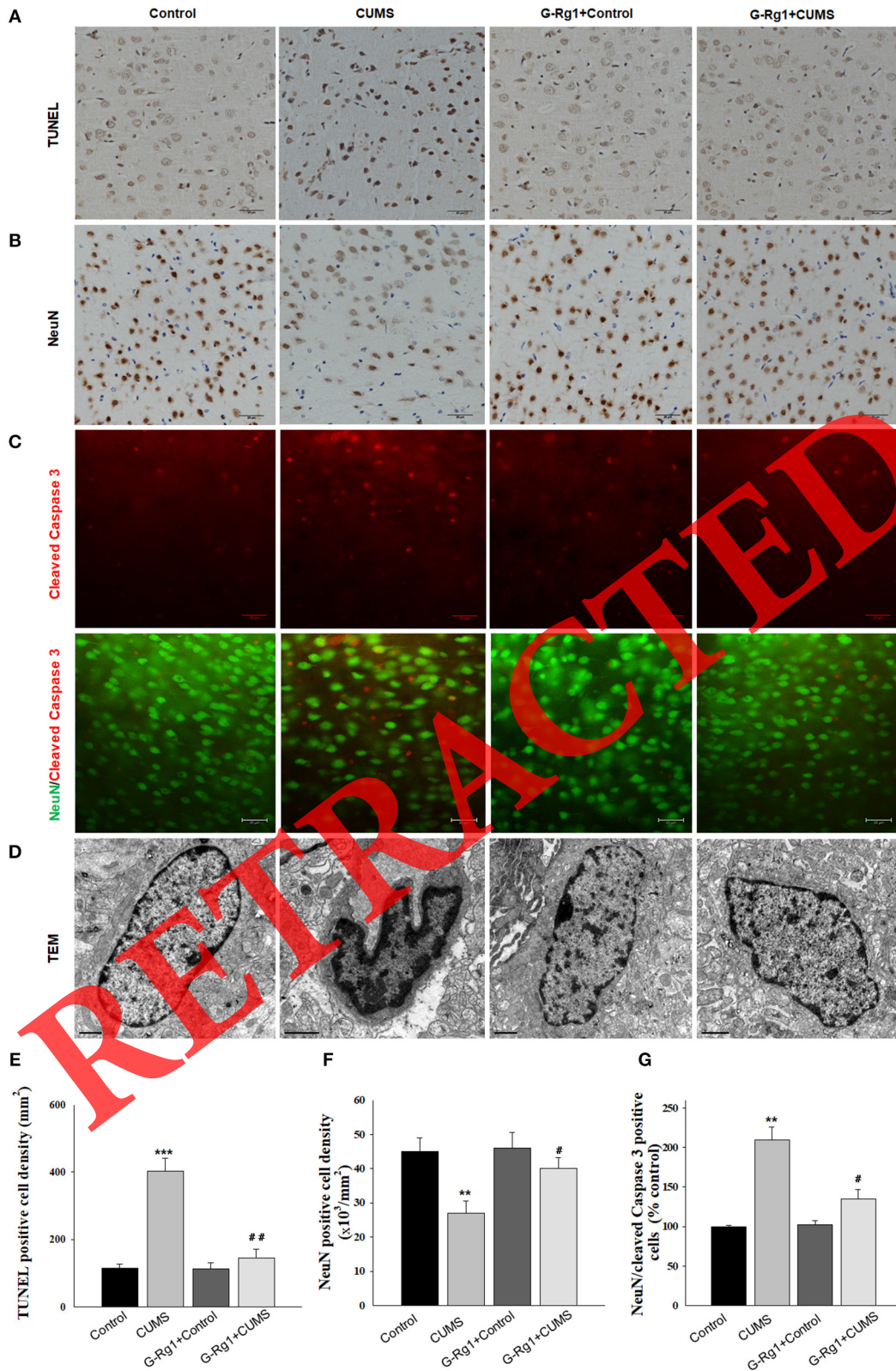


**FIGURE 7 |** Ginsenoside-Rg1 reduced neuronal apoptosis within the vmPFC region as induced by CUMS-exposure. **(A)** Representative images of TUNEL staining from the vmPFC region. Scale bar is 20  $\mu$ m. *N* = 4 per group. **(B)** Representative images of immunohistochemical staining of NeuN expression within the vmPFC  
(Continued)

**FIGURE 7** | region. Scale bar is 20  $\mu\text{m}$ . *N* = 4 per group. **(C)** Representative images of immunofluorescence staining of NeuN/cleaved Caspase 3 double labeled positive cells within the vmPFC region. Scale bar is 20  $\mu\text{m}$ . *N* = 4 per group. **(D)** Representative electron micrograph of vmPFC neuronal ultrastructure revealing nuclear chromatin aggregation, condensation and margination. Scale bar is 1  $\mu\text{m}$ . **(E)** Bar graphs show quantification of TUNEL positive cells density in the vmPFC region. **(F)** Bar graphs show quantification of NeuN positive cells density in the vmPFC region. **(G)** Bar graphs show quantification of NeuN/cleaved Caspase 3 positive cells in the vmPFC region. *N* = 6 per group. Data were presented as the means  $\pm$  SEM. \*\**P* < 0.01, \*\*\**P* < 0.001 CUMS vs. Control group; #*P* < 0.05, ##*P* < 0.01 G-Rg1+CUMS vs. CUMS group. G-Rg1, Ginsenoside-Rg1.

increased expression levels of Caspase-3 and Caspase-9, along with the decreased expression levels of Bcl-2 within the vmPFC which resulted from CUMS exposure (*P* < 0.01) (**Figure 8D**).

## DISCUSSION

Depression has become one of the most prevalent psychiatric disorders and imposes a substantial societal burden (31, 32). Classical antidepressants currently used for treatment of depression usually induce many side effects and possess low efficacy (33). There exists evidence indicating a potential role for ginsenoside-Rg1 in the treatment of depression (34), although the mechanisms have yet to be determined. In this study, our findings demonstrate that ginsenoside-Rg1 ameliorated behavioral dysfunctions induced by chronic stress via attenuating activation of microglia and astrocytes as well as by decreasing the overexpression in a series of pro-inflammatory cytokines, decreasing structural deficits in dendritic spines and synapses and ameliorating neuronal apoptosis within the vmPFC. These processes may then represent significant mechanistic components responsible for the antidepressant effects of ginsenoside-Rg1 via suppressing neurodegeneration in vmPFC region.

The CUMS-induced animal model of depression is widely used for investigating the underlying mechanisms of depression and for screening the efficacy of antidepressants as assessed with use of behavioral tests indicative of depression (35, 36). Our behavioral assays show that CUMS induces depression-like behaviors in rats as revealed in the sucrose preference and forced swim tests, results which were similar to those of previous reports (37, 38). These CUMS-induced behavioral responses were prevented with chronic pretreatment of ginsenoside-Rg1, suggesting that ginsenoside-Rg1 treatment exerts antidepressant-like effects in this CUMS-induced animal model of depression.

More importantly, in this report, we examined several potential mechanistic bases for this antidepressant-like effect. One of the main findings was the anti-inflammatory effects exerted by ginsenoside-Rg1 in response to chronic stress as demonstrated by the suppression of microglia and astrocytic activation in vmPFC regions. Neuroinflammation plays a critical role in the pathogenesis of various neurological disorders including depression (7, 39). As microglia is the resident immune cell in brain, they normally respond to various neuropathological stimuli, including stress, injury, and infection (40). Once activated, a rapid proliferation in microglia densities and morphological changes result, followed by the release of pro-inflammatory cytokines, such as IL-1, TNF- $\alpha$ , and IFN- $\gamma$ . This cascade then contributes to neuronal damage, cell death and astroglial activation, all of which represent possible factors

associated with major depressive disorder (41, 42). It was reported that in depressed patients, elevated microglia activation is associated with individuals who committed suicide (43, 44). Interestingly, one of the mechanisms of antidepressant treatment may involve reductions in microglial activation and serum levels of IL-1 $\beta$ , suggesting that pro-inflammatory cytokines can be used as a potential targets in the treatment of depression (45–47). Astrocyte is another important immune cell which occurs in response to pathological stimuli. In addition to these effects of microglia, astrocyte activation also results in release of some neurotoxic factors, for example cytokines. Accordingly, prevention of reactive astrogliosis is becoming a critical issue in the development of therapeutic interventions for brain injury (48, 49). Consistently, the findings of our current study show that in this chronic stress-induced model of depression, the presence of depression-like behaviors was associated with elevations in microglial and astrocytic activation within the vmPFC. Chronic stress increased inflammatory cytokines and GFAP expression levels within the vmPFC, an effect which was associated with cellular hypertrophy of microglia and astrocytes. However, our current findings demonstrating that chronic ginsenoside-Rg1 treatment significantly suppressed inflammatory cytokine levels as well as microglial activation. In addition, in the present study, we also found ginsenoside-Rg1 could decreased CUMS exposure-induced astroglial activation and reduced GFAP expression in vmPFC region.

It should be noted that, ginsenoside Rg1 was also reported showing anti-inflammation effects in other brain areas which associated with depression. For example, ginsenoside Rg1 inhibited the inflammation mediated by LPS via suppressing NF $\kappa$ B and MAPK pathway in both cerebral cortex and hippocampus (50). In addition, previous studies provide evidence that ginsenoside Rg1 can improve cognitive ability by enhancing the antioxidant and anti-inflammatory capacity in the hippocampus (23). Moreover, in our previous study, we also found that ginsenoside Rg1 reverses chronic stress-induced depression-like behaviors, BDNF expression and the phosphorylation levels of PKA and CREB in amygdala, another important brain area associated with depression (15). These results demonstrated that ginsenoside-Rg1 appears to be a multi-target natural compound that may modulate numerous pathways, of which detailed characterization of the neuronal mechanisms worthy of study. For this depression animal model used in the present study, we suspect that ginsenoside-Rg1 may also exert neuroprotective effects in dentate gyrus and CA1 regions of hippocampus. Taken together, our results provide strong evidence that ginsenoside-Rg1 might exert antidepressant-like effects through attenuating inflammation responses.

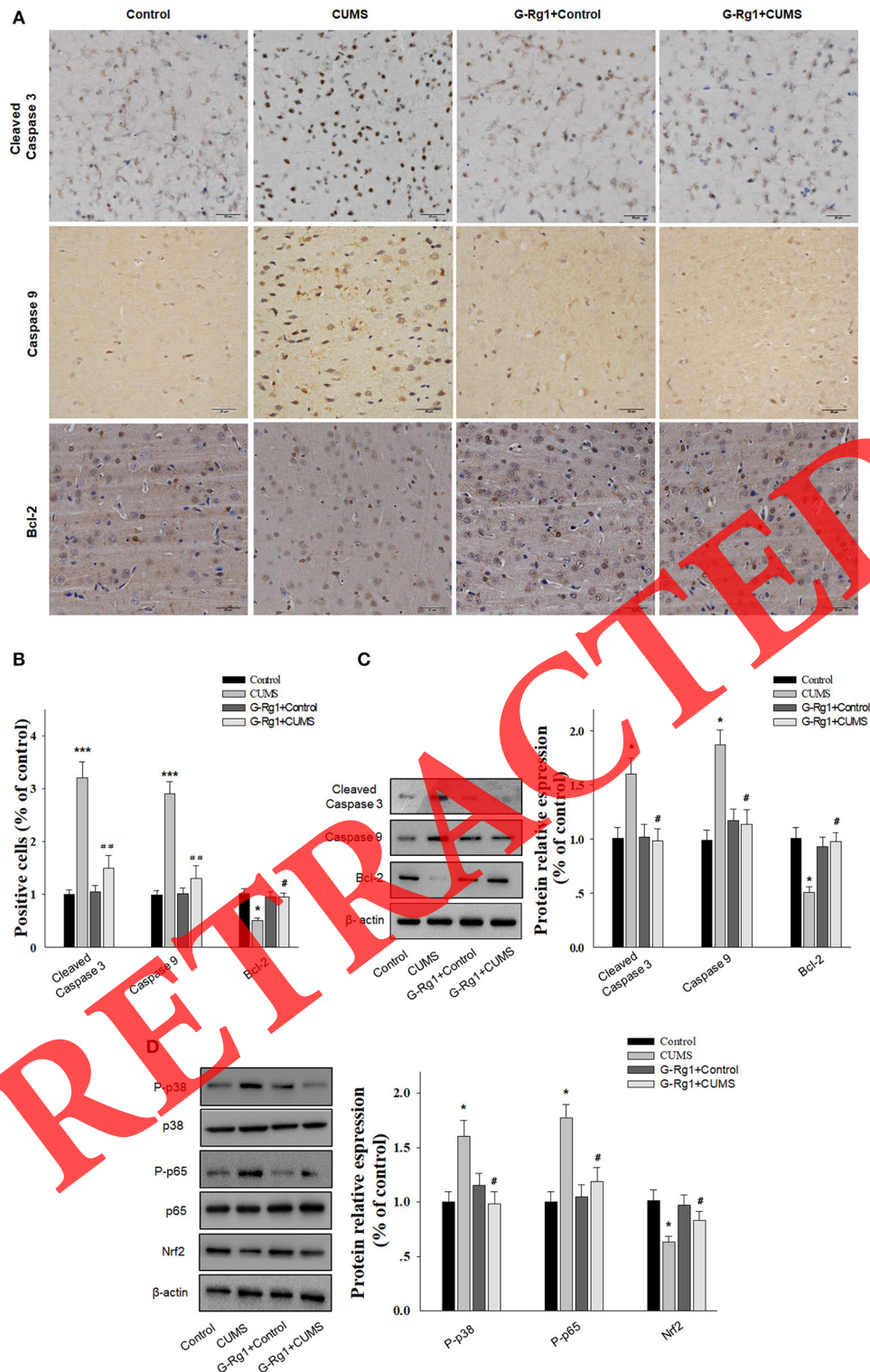


**FIGURE 8 |** Ginsenoside-Rg1 suppressed the expression of apoptosis-related proteins within the vmPFC region as induced by CUMS-exposure. **(A)** Expression of cleaved caspase-3, caspase-9, and Bcl-2 within with the vmPFC region with use of immunohistochemical staining. Scale bar is 20  $\mu$ m. **(B)** Bar graphs show quantification of cleaved caspase-3, caspase-9, and Bcl-2. Values are expressed relative to those of the control group. **(C)** Expression of cleaved caspase-3, caspase-9, and Bcl-2 within with the vmPFC region with use of Western Blot assays. **(D)** Expression of phosphorylated p38, p65, and Nrf2 within with the vmPFC region with use of Western Blot assays. *N* = 6 per group. Data were presented as the means  $\pm$  SEM. \**P* < 0.05, \*\*\**P* < 0.001 CUMS vs. Control group; #*P* < 0.05, ##*P* < 0.01 G-Rg1+CUMS vs. CUMS group. G-Rg1, Ginsenoside-Rg1.

Depression is considered associated with structural and functional injuries within specific brain regions (51). Dendrite aberration is a common feature of stress-related neurodegenerative diseases, but the underlying mechanisms remain largely elusive. Recent evidence has demonstrated that impairments in neuroplasticity are mediated through various neuroimmune mechanisms under pathophysiological conditions associated with depression (52–54). In the present study, we evaluated the effects of chronic stress and pretreatment with ginsenoside-Rg1 on neuronal dendritic spine morphology and the expression of a variety of key regulators of synaptic structure in rats. Here, we show that chronic stress resulted in defective terminal dendrite spine density accompanied by a loss of spines and synapses. Such reductions in input to plasma membranes of vmPFC neurons would likely result in the synaptic transmission deficiencies and thus behavioral changes. Synaptophysin and PSD-95 are now well accepted as being scaffolding proteins that have been implicated in the regulation of synapse function. In our current study, the stress-induced changes in spine synapse number were accompanied with a decrease in the specific dendritic spine protein, synaptophysin, as well as in levels of the postsynaptic protein, PSD-95. In addition, some important synaptic plasticity-related regulating proteins, such as CREB and BDNF, were also subject to modulation by the chronic stress paradigm. More importantly, ginsenoside-Rg1 treatment significantly ameliorated these decreased spine synaptic densities and expression levels of synaptic-related proteins, effects that were associated with improving behavioral deficits resulting from chronic stress. Recent evidence has implicated that ginsenoside Rg1 promotes the neural differentiation via upregulation of miRNA-124 expression (55), as well as promotes angiogenesis possibly through the modulation of miRNA-214 and miRNA-23a expression (56, 57). Similarly, in our recent studies, we found that miR-134-mediated deficits of spine synapse may be related to the depression-like behaviors in stressed rats, and ginsenoside-Rg1 could prevent the overexpression of miR-134 in vmPFC induced by chronic stress (58). It is suggested that the transcription factor CREB and BDNF are two important potential targets of miRNA-134 which could inhibit the translation of mRNAs of these plasticity-associated proteins. Ginsenoside-Rg1 is a natural steroidal saponin which suggested could across biological membranes. Therefore, we proposed that ginsenoside-Rg1 may up-regulate the expression of CREB and BDNF via preventing the suppressive effects of miRNA-134 on their mRNA, and thus ameliorated the dendrite synaptic deficits. Therefore, these results suggest that ginsenoside-Rg1 regulates structural deficits of spine synapses in response to chronic stress through its neuroprotective properties and may thus induce antidepressant-like effects.

Aside from neuroinflammation and synaptic deterioration as described above, additional critical mechanisms underlying the neuroprotective effects of ginsenoside-Rg1 against depression-like behaviors were also investigated in the present study. Inflammatory cytokines are now considered as important pro-apoptotic factors involved in the progression of neurological disorders (59). For example, intra-striatal IL-1 $\beta$  administration in rats, which triggers inflammatory responses, is subsequently

accompanied with increased apoptosis 24 h post-injection, an effect which then promotes brain injury (60). In the present study, we found that the depression-like symptoms observed in rats following chronic stress were accompanied by a marked increasing in neuronal apoptosis within vmPFC regions. These findings reveal a new potential mechanism through which chronic stress can induce brain injury. In support of this eventuality are our current results demonstrating that CUMS exposure significantly increases the number of TUNEL positive apoptotic cells in this area. Moreover, the double labeling experiments with NeuN and cleaved caspase 3 also confirmed that the neuronal cell population undergoing apoptosis after chronic stress. Furthermore, ultrastructural changes reveal that nuclear chromatin margination and nuclear karyopyknosis were clearly present in apoptotic cells of rats subjected to CUMS exposure. Recent studies in our laboratory have shown that chronic stress induced microglial activation and overexpression of the pro-inflammatory cytokine IL-1 $\beta$  in vmPFC region, while pretreatment of IL-1 $\beta$  antagonists significantly ameliorated the deficits of neuronal structure, as well as repressed the display of depression-like behaviors induced by CUMS (61). These results suggested that neuroinflammatory responses may cause the neuronal structural changes and in turn the cell death in depression animal models induced by chronic stress. Reverse, the increased neuronal cell loss may further strengthen the inflammatory responses, this interaction let them worked synergistically to cause the depression-like behaviors.

Previous studies have reported that ginsenoside Rg1 could protect against inflammation and neuron apoptosis in hippocampus region in cerebral ischemia-reperfusion rats by activating PPAR $\gamma$ /HO-1 signaling pathway (62, 63). While, to our knowledge, there exists no evidence indicating any anti-apoptotic effects of ginsenoside-Rg1 as related to its anti-depression effects, in this study, we now show that chronic ginsenoside-Rg1 treatment significantly suppressed neuronal apoptosis in vmPFC region induced by stress in this rat model of depression. These effects likely involve the downregulation in the activation of pro-apoptotic proteins, Bak, Caspase-3, and Caspase-9, and an upregulation in the anti-apoptotic protein, Bcl-2, within the vmPFC of stressed rats. Notably, this anti-apoptosis capacity of ginsenoside-Rg1 treatment might represent one of its most pivotal components responsible for the beneficial recovery in depressive phenotypes. Therefore, these findings not only confirm the neuroprotective effects of ginsenoside-Rg1 in this CUMS-induced depression model but offer new insights into the mechanistic basis for this neuroprotection, namely through its ability to promote anti-apoptosis.

Recently, increasing evidence has revealed that the MAPK pathway represents an important signal transduction pathway in the regulation of inflammation and apoptosis (64). The studies reported that the pro-inflammatory factor IL-1 $\beta$  could activate p38 MAPK cascades (65) and has been shown to induce robust neuronal apoptosis resulting in neuronal injury within the rat hippocampus (66). Our present results showed that chronic stress significantly increased the expression of phosphorylation levels of p38 MAPK within the vmPFC region that could be significantly reversed by ginsenoside-Rg1.



It is considered that the released inflammatory factors can activate amplification of NF- $\kappa$ B activity, then the nuclear translocation of NF- $\kappa$ B p65 subunit subsequently leads to further gene expression of various pro-inflammatory cytokines in a regulatory cycle. As a result, the activation of NF- $\kappa$ B triggered expression of pro-apoptotic factor genes, which ultimately leads to apoptosis and neural cell death (67). Previous studies have demonstrated that ginsenoside-Rg1 could protect hepatocytes against excessive inflammation and hepatocellular apoptosis via preventing the NF- $\kappa$ B pathway (68–70) and may prevent against acute liver injury by activating Nrf2 signaling pathway in mice (71). Consistently, in the present study, we found that pretreatment of ginsenoside-Rg1 significantly reversed the increased phosphorylation levels of NF- $\kappa$ B P65 subunit, as well as reversed the decreased expression of Nrf2 within the vmPFC of these CUMS rats. Taken together, these results suggest that ginsenoside-Rg1 may exert neuroprotective effects through activating Nrf2 signaling pathway and inhibits NF- $\kappa$ B and p38 MAPK activation to reduce neuronal inflammation and apoptosis in CUMS-induced depressive rats. However, detailed molecular mechanisms regarding the means through which chronic stress may induce neuroninflammation and apoptosis will require further investigation.

In summary, these results provide strong evidence enabling us to identify some of the potential neuroprotective mechanisms of ginsenoside-Rg1 as related to the treatment of depression. Specifically, we show that this agent exerts: (1) anti-inflammatory effects by modulating glial activation and pro-inflammatory cytokines expression, (2) amelioration of neuronal structural changes by suppressing deficits of spines and synapses, and (3)

anti-apoptosis effects by preventing pro-apoptotic protein levels within localized neuronal sites. Taken together, these findings not only reveal some of the underlying mechanisms for ginsenoside-Rg1's neuroprotective effects against neurodegeneration but also provide proposals for novel therapeutic approaches in the treatment of depression.

## AUTHOR CONTRIBUTIONS

SY: Experiments design, paper writing, and data analysis. CF: Animal behavior tests, Western blot analysis, TUNEL staining, and RT-PCR. QS: Electron microscope analysis and stereotatic injection. PW: qPCR and ELISA. YL: Animal behavior experiments. MY: depression model and Western blot analysis.

## ACKNOWLEDGMENTS

This study was supported by grants to SY from the National Natural Science Foundation of China (NSFC81873796; NSFC81471371), Shandong Provincial Key Research and Development Plan (2017CXGC1504), the Fundamental Research Funds of Shandong University (2018JC008), and the Key Research and Development Foundation of Shandong Province (2018GSP118050).

## SUPPLEMENTARY MATERIAL

The Supplementary Material for this article can be found online at: <https://www.frontiersin.org/articles/10.3389/fimmu.2018.02889/full#supplementary-material>

## REFERENCES

- Vyas A, Mitra R, Shankaranarayana Rao BS, Chattarji S. Chronic stress induces contrasting patterns of dendritic remodeling in hippocampal and amygdaloid neurons. *J Neurosci.* (2002) 22:6810–8. doi: 10.1523/JNEUROSCI.22-15-06810.2002
- Stockmeier CA, Mahajan GL, Konick LC, Overholser JC, Jurjus GJ, Meltzer HY, et al. Cellular changes in the postmortem hippocampus in major depression. *Biol Psychiatry* (2004) 56:640–50. doi: 10.1016/j.biopsych.2004.08.022
- Oh DH, Son H, Hwang S, Kim SH. Neuropathological abnormalities of astrocytes, GABAergic neurons, and pyramidal neurons in the dorsolateral prefrontal cortices of patients with major depressive disorder. *Eur Neuropsychopharmacol.* (2012) 22:330–8. doi: 10.1016/j.euroneuro.2011.09.001
- Tan MS, Yu JT, Jiang T, Zhu XC, Tan L. The NLRP3 inflammasome in Alzheimer's disease. *Mol Neurobiol.* (2013) 48:875–82. doi: 10.1007/s12035-013-8475-x
- Zhang N, Zhang X, Liu X, Wang H, Xue J, Yu J. Chrysophanol inhibits NALP3 inflammasome activation and ameliorates cerebral ischemia/reperfusion in mice. *Mediat Inflamm.* (2014) 2014:370530. doi: 10.1155/2014/370530
- Liu HD, Li W, Chen ZR, Hu YC, Zhang DD, Shen W, et al. Expression of the NLRP3 inflammasome in cerebral cortex after traumatic brain injury in a rat model. *Neurochem Res.* (2013) 38:2072–83. doi: 10.1007/s11064-013-1115-z
- Dowlati Y, Herrmann N, Swardfager W, Liu H, Sham L, Reim EK, et al. A meta-analysis of cytokines in major depression. *Biol Psychiatry* (2010) 67:446–57. doi: 10.1016/j.biopsych.2009.09.033
- Schiepers OJ, Wichers MC, Maes M. Cytokines and major depression. *Prog Neuropsychopharmacol Biol Psychiatry* (2005) 29:201–17. doi: 10.1016/j.pnpbp.2004.11.003
- Song C, Halbreich U, Han C, Leonard BE, Luo H. Imbalance between pro- and anti-inflammatory cytokines and between Th1 and Th2 cytokines in depressed patients: the effect of electroacupuncture or fluoxetine treatment. *Pharmacopsychiatry* (2009) 42:182–8. doi: 10.1055/s-0029-1202263
- Maes M, Song C, Yirmiya R. Targeting IL-1 in depression. *Expert Opin Ther Targets* (2012) 16:1097–12. doi: 10.1517/14728222.2012.718331
- Rawdin BJ, Mellon SH, Dhabhar FS, Epel ES, Puterman E, Su Y. Dysregulated relationship of inflammation and oxidative stress in major depression. *Brain Behav Immun.* (2013) 31:143–52. doi: 10.1016/j.bbi.2012.11.011
- Cook SC, Wellman CL. Chronic stress alters dendritic morphology in rat medial prefrontal cortex. *J Neurobiol.* (2004) 60:236–48. doi: 10.1002/neu.20025
- Goldwater DS, Pavlides C, Hunter RG, Bloss EB, Hof PR, McEwen B, et al. Structural and functional alterations to rat medial prefrontal cortex following chronic restraint stress and recovery. *Neuroscience* (2009) 164:798–808. doi: 10.1016/j.neuroscience.2009.08.053
- Zhang L, Luo JX, Zhang M, Yao W, Ma X, Yu SY. Effects of curcumin on chronic unpredictable mild stress-induced depressive-like behavior and structural plasticity in the lateral amygdala of rats. *Int J Neuropsychopharmacol.* (2014) 17:793–806. doi: 10.1017/S1461145713001661
- Liu Z, Qi Y, Cheng Z, Zhu X, Fan C, Yu SY. The effects of ginsenoside Rg1 on chronic stress induced depression-like behaviors, BDNF expression and the phosphorylation of PKA and CREB in rats. *Neuroscience* (2016) 322:358–69. doi: 10.1016/j.neuroscience.2016.02.050

16. Rust MB. Novel functions for ADF/cofilin in excitatory synapses - lessons from gene-targeted mice. *Commun Integrat Biol.* (2015) 8:e1114194. doi: 10.1080/19420889.2015.1114194
17. Liu A, Zhou Z, Dang R, Zhu Y, Qi J, He G, et al. Neuroligin 1 regulates spines and synaptic plasticity via LIMK1/cofilin-mediated actin reorganization. *J Cell Biol.* (2016) 212:449–63. doi: 10.1083/jcb.201509023
18. Zhang Q, Gao X, Li C, Feliciano C, Wang D, Zhou D, et al. Impaired dendritic development and memory in Sorbs2 knock-out mice. *J Neurosci.* (2016) 36:2247–60. doi: 10.1523/JNEUROSCI.2528-15.2016
19. Lee SE, Kim Y, Han JK, Park H, Lee U, Na M, et al. nArgBP2 regulates excitatory synapse formation by controlling dendritic spine morphology. *Proc Natl Acad Sci USA.* (2016) 113:6749–54. doi: 10.1073/pnas.1600944113
20. Zhang X, Wang J, Xing Y, Gong L, Li H, Wu Z, et al. Effects of ginsenoside Rg1 or 17 $\beta$ -estradiol on a cognitively impaired, ovariectomized rat model of Alzheimer's disease. *Neuroscience* (2012) 220:191–200. doi: 10.1016/j.neuroscience.2012.06.027
21. Song XY, Hu JF, Chu SF, Zhang Z, Xu S, Yuan YH, et al. Ginsenoside Rg1 attenuates okadaic acid induced spatial memory impairment by the GSK3 $\beta$ /tau signaling pathway and the A $\beta$  formation prevention in rats. *Eur J Pharmacol.* (2013) 710:29–38. doi: 10.1016/j.ejphar.2013.03.051
22. Wang Y, Kan H, Yin Y, Wu W, Hu W, Wang M, et al. Protective effects of ginsenoside Rg1 on chronic restraint stress induced learning and memory impairments in male mice. *Pharmacol Biochem Behav.* (2014) 120:73–81. doi: 10.1016/j.pbb.2014.02.012
23. Zhu J, Mu X, Zeng J, Xu C, Liu J, Zhang M, et al. Ginsenoside Rg1 prevents cognitive impairment and hippocampus senescence in a rat model of D-galactose-induced aging. *PLoS ONE* (2014) 9:e101291. doi: 10.1371/journal.pone.0101291
24. Zhu X, Rui G, Liu Z, Cheng Z, Qi Y, Fan C, Yu SY. Ginsenoside Rg1 reverses stress-induced depression-like behaviors and BDNF expression within the prefrontal cortex. *Eur J Neurosci.* (2016) 44:1878–85. doi: 10.1111/ejn.13255
25. Holmes A, Wellman CL. Stress-induced prefrontal reorganization and executive dysfunction in rodents. *Neurosci Biobehav Rev.* (2009) 33:773–83. doi: 10.1016/j.neubiorev.2008.11.005
26. McLaughlin KJ, Baran SE, Conrad CD. Chronic stress- and sex-specific neuromorphological and functional changes in limbic structures. *Mol Neurobiol.* (2009) 40:166–82. doi: 10.1007/s12035-009-8079-7
27. Mao QQ, Ip SP, Ko KM, Tsai SH, Che CT. Peony glycosides produce antidepressant-like action in mice exposed to chronic unpredictable mild stress: effects on hypothalamic-pituitary-adrenal function and brain-derived neurotrophic factor. *Prog Neuropsychopharmacol Biol Psychiatry* (2009) 33:1211–6. doi: 10.1016/j.pnpbp.2009.07.002
28. Porsolt RD, Le Pichon M, Jalfre M. Depression: a new animal model sensitive to antidepressant treatments. *Nature* (1977) 266:730–2. doi: 10.1038/266730a0
29. Duman CH, Schlesinger L, Kodama M, Russell DS, Duman RS. A role for MAP kinase signaling in behavioral models of depression and antidepressant treatment. *Biol Psychiatry* (2007) 61:661–70. doi: 10.1016/j.biopsych.2006.05.047
30. Wang Y, Huang Y, Xu Y, Ruan W, Wang H, Zhang Y, et al. A dual AMPK/Nrf2 activator reduces brain inflammation after stroke by enhancing microglia M2 polarization. *Antioxid Redox Signal.* (2017) 28:141–63. doi: 10.1089/ars.2017.7003
31. Lépine J-P, Briley M. The increasing burden of depression. *Neuropsychiatr. Dis Treat* (2011) 7:3–7. doi: 10.2147/NDT.S19617
32. Hidaka BH. Depression as a disease of modernity: explanations for increasing prevalence. *J Affect Disord.* (2012) 140:205–14. doi: 10.1016/j.jad.2011.12.036
33. Andrews PW, Bharwani A, Lee KR, Fox M, Thomson JA Jr. Is serotonin an upper or a downer? The evolution of the serotonergic system and its role in depression and the antidepressant response. *Neurosci Biobehav Rev.* (2015) 51:164–88. doi: 10.1016/j.neubiorev.2015.01.018
34. Jiang B, Xiong Z, Yang J, Wang W, Wang Y, Hu ZL, et al. Antidepressant-like effects of ginsenoside Rg1 are due to activation of the BDNF signalling pathway and neurogenesis in the hippocampus. *Br J Pharmacol.* (2012) 166:1872–87. doi: 10.1111/j.1476-5381.2012.01902.x
35. Schmidt HD, Shelton RC, Duman RS. Functional biomarkers of depression: diagnosis, treatment, and pathophysiology. *Neuropsychopharmacology* (2011) 36:2375–94. doi: 10.1038/npp.2011.151
36. Christiansen SH, Olesen MV, Wörtwein G, Woldbye DP. Fluoxetine reverts chronic restraint stress-induced depression-like behaviour and increases neuropeptide Y and galanin expression in mice. *Behav Brain Res.* (2011) 216:585–91. doi: 10.1016/j.bbr.2010.08.044
37. Willner P. Chronic mild stress (CMS) revisited: consistency and behavioural-neurobiological concordance in the effects of CMS. *Neuropsychobiology* (2005) 52:90–110. doi: 10.1159/000087097
38. Zhao Z, Wang W, Guo H, Zhou D. Antidepressant-like effect of liquiritin from *Glycyrrhiza uralensis* in chronic variable stress induced depression model rats. *Behav Brain Res.* (2008) 94:108–13. doi: 10.1016/j.bbr.2008.06.030
39. Alcocer-Gomez E, Ulecia-Moron C, Marin-Aguilar F, Rybkina T, Casas-Barquero N, Ruiz-Cabello J, et al. Stress-induced depressive behaviors require a functional NLRP3 inflammasome. *Mol Neurobiol.* (2015) 53:4874–82. doi: 10.1007/s12035-015-9408-7
40. Dheen ST, Kaur C, Ling EA. Microglial activation and its implications in the brain diseases. *Curr Med Chem.* (2007) 14:1189–97. doi: 10.2174/092986707780597961
41. Pan Y, Chen XY, Zhang QY, Kong LD. Microglial NLRP3 inflammasome activation mediates IL-1 $\beta$ -related inflammation in prefrontal cortex of depressive rats. *Brain Behav Immun.* (2014) 41:90–100. doi: 10.1016/j.bbi.2014.04.007
42. Fernanda NK, Ana PC, Gabriele G, Alexandre PD, Ana Lúcia SR, Hugo P, Manuella PK. NLRP3 inflammasome-driven pathways in depression: clinical and preclinical findings. *Brain Behav Immun.* (2017) 64:367–83. doi: 10.1016/j.bbi.2017.03.002
43. Steiner J, Bielau H, Brisch R, Danos P, Ullrich O, Mawrin C, et al. Immunological aspects in the neurobiology of suicide: elevated microglial density in schizophrenia and depression is associated with suicide. *J Psychiatr Res.* (2008) 42:151–7. doi: 10.1016/j.jpsychires.2006.10.013
44. Schnieder TP, Trencsevska I, Rosoklija G, Stankov A, Mann JJ, Smiley J, et al. Microglia of prefrontal white matter in suicide. *J Neuropathol Exp Neurol.* (2014) 73:880–90. doi: 10.1097/NEN.0000000000000107
45. Hannestad J, DellaGioia N, Bloch M. The effect of antidepressant medication treatment on serum levels of inflammatory cytokines: a metaanalysis. *Neuropsychopharmacology* (2011) 36:2452–9. doi: 10.1038/npp.2011.132
46. Lee JY, Kang SR, Yune TY. Fluoxetine prevents oligodendrocyte cell death by inhibiting microglia activation after spinal cord injury. *J Neurotrauma* (2015) 32:633–44. doi: 10.1089/neu.2014.3527
47. Du RH, Tan J, Sun XY, Lu M, Ding JH, Hu G. Fluoxetine inhibits NLRP3 inflammasome activation: implication in depression. *Int J Neuropsychopharmacol.* (2016) 19:pyw037. doi: 10.1093/ijnp/pyw037
48. Sofroniew MV, Vinters HV. Astrocytes: biology and pathology. *Acta Neuropathol.* (2010) 119:7–35. doi: 10.1007/s00401-009-0619-8
49. Pekny M, Pekna M. Astrocyte reactivity and reactive astrogliosis: costs and benefits. *Physiol. Rev.* (2014) 94:1077–98. doi: 10.1152/physrev.00041.2013
50. Hu JF, Song XY, Chu SF, Chen J, Ji HJ, Chen XY, et al. Inhibitory effect of ginsenoside Rg1 on lipopolysaccharide-induced microglial activation in mice. *Brain Res.* (2011) 1374:8–14. doi: 10.1016/j.brainres.2010.11.069
51. Gilabert-Juan J, Castillo-Gomez E, Pérez-Rando M, Moltó MD, Nacher J. Chronic stress induces changes in the structure of interneurons and in the expression of molecules related to neuronal structural plasticity and inhibitory neurotransmission in the amygdala of adult mice. *Exp Neurol.* (2011) 232:33–40. doi: 10.1016/j.expneurol.2011.07.009
52. Garcia-Bueno B, Caso JR, Leza JC. Stress as a neuroinflammatory condition in brain: damaging and protective mechanisms. *Neurosci Biobehav Rev.* (2008) 32:1136–51. doi: 10.1016/j.neubiorev.2008.04.001
53. Anisman H. Cascading effects of stressors and inflammatory immune system activation: implications for major depressive disorder. *J Psychiatry Neurosci.* (2009) 34:4–20.
54. Kubera M, Obuchowicz E, Goehler L, Brzeszcz J, Maes M. In animal models, psychosocial stress-induced (neuro) inflammation, apoptosis and reduced neurogenesis are associated to the onset of depression. *Prog Neuropsychopharmacol Biol Psychiatry* (2010) 35:744–59. doi: 10.1016/j.pnpbp.2010.08.026
55. Dong J, Zhu G, Wang TC, Shi FS. Ginsenoside Rg1 promotes neural differentiation of mouse adipose-derived stem cells via the miRNA-124 signaling pathway. *J Zhejiang Univ Sci B* (2017) 8:445–8. doi: 10.1631/jzus.B1600355

56. Chan LS, Yue PY, Mak NK, Wong RN. Role of microRNA-214 in ginsenoside-Rg1-induced angiogenesis. *Eur J Pharm Sci.* (2009) 38:370–7. doi: 10.1016/j.ejps.2009.08.008
57. Kwok HH, Chan LS, Poon PY, Yue PY, Wong RN. Ginsenoside-Rg1 induces angiogenesis by the inverse regulation of MET tyrosine kinase receptor expression through miR-23a. *Toxicol Appl Pharmacol.* (2015) 287:276–83. doi: 10.1016/j.taap.2015.06.014
58. Fan C, Zhu X, Song Q, Wang P, Liu Z, Yu SY. MiR-134 modulates chronic stress-induced structural plasticity and depression-like behaviors via downregulation of Limk1/cofilin signaling in rats. *Neuropharmacology* (2018) 131:364–76. doi: 10.1016/j.neuropharm.2018.01.009
59. Tsai SJ. Effects of interleukin-1beta polymorphisms on brain function and behavior in healthy and psychiatric disease conditions. *Cytokine Growth Factor Rev.* (2017) 37:89–97. doi: 10.1016/j.cytogfr.2017.06.001
60. Griffin ÉW, Yssel JD, O'Neill E, Ryan KJ, Boyle N, Harper P, et al. The  $\beta$ 2-adrenoceptor agonist clenbuterol reduces the neuroinflammatory response, neutrophil infiltration and apoptosis following intra-striatal IL-1 $\beta$  administration to rats. *Immunopharmacol Immunotoxicol.* (2018) 40:99–106. doi: 10.1080/08923973.2017.1418882
61. Fan C, Song Q, Wang P, Li Y, Yang M, Liu B, et al. Curcumin protects against chronic stress-induced dysregulation of neuroplasticity and depression-like behaviors via suppressing IL-1 $\beta$  pathway in rats. *Neuroscience* (2018) 392:92–106 doi: 10.1016/j.neuroscience.2018.09.028
62. Yang Y, Li X, Zhang L, Liu L, Jing G, Cai H. Ginsenoside Rg1 suppressed inflammation and neuron apoptosis by activating PPAR $\gamma$ /HO-1 in hippocampus in rat model of cerebral ischemia-reperfusion injury. *Int J Clin Exp Pathol.* (2015) 8:2484–94.
63. Li Y, Guan Y, Wang Y, Yu CL, Zhai FG, Guan LX. Neuroprotective effect of the ginsenoside Rg1 on cerebral ischemic injury *in vivo* and *in vitro* is mediated by PPAR $\gamma$ -regulated antioxidative and anti-inflammatory pathways. *Evid Based Complement Alternat Med.* (2017) 2017:7842082. doi: 10.1155/2017/7842082
64. Kim EK, Choi EJ. Compromised MAPK signaling in human diseases: an update. *Arch Toxicol.* (2015) 89:867–82. doi: 10.1007/s00204-015-1472-2
65. Yu J, Berga SL, Zou W, Yook DG, Pan JC, Andrade AA, et al. IL-1 $\beta$  inhibits connexin 43 and disrupts decidualization of human endometrial stromal cells through ERK1/2 and p38 MAP kinase. *Endocrinology* (2017) 158:4270–85. doi: 10.1210/en.2017-00495
66. Dong Y, Kalueff AV, Song C. N-methyl-d-aspartate receptor-mediated calcium overload and endoplasmic reticulum stress are involved in interleukin-1beta-induced neuronal apoptosis in rat hippocampus. *J Neuroimmunol.* (2017) 307:7–13. doi: 10.1016/j.jneuroim.2017.03.005
67. De Lucca FL, Serrano SV, Souza LR, Watanabe MA. Activation of RNA-dependent protein kinase and nuclear factor-kB by regulatory RNA from lipopolysaccharide-stimulated macrophages: implications for cytokine production. *Eur J Pharmacol.* (2002) 450:85–9. doi: 10.1016/S0014-2999(02)02072-1
68. Ni XJ, Xu ZQ, Jin H, Zheng SL, Cai Y, Wang JJ. Ginsenoside Rg1 protects human renal tubular epithelial cells from lipopolysaccharide-induced apoptosis and inflammation damage. *Braz J Med Biol Res.* (2017) 51:e6611. doi: 10.1590/1414-431x20176611
69. Li J, Yang C, Zhang S, Liu S, Zhao L, Luo H, et al. Ginsenoside Rg1 inhibits inflammatory responses via modulation of the nuclear factor-kB pathway and inhibition of inflammasome activation in alcoholic hepatitis. *Int J Mol Med.* (2018) 41:899–907. doi: 10.3892/ijmm.2017.3297
70. Qi B, Zhang S, Guo D, Guo S, Jiang X, Zhu X. Protective effect and mechanism of ginsenoside Rg1 on carbon tetrachloride-induced acute liver injury. *Mol Med Rep.* (2017) 16:2814–22. doi: 10.3892/mmr.2017.6920
71. Ning C, Gao X, Wang C, Huo X, Liu Z, Sun H, et al. Hepatoprotective effect of ginsenoside Rg1 from Panax ginseng on carbon tetrachloride-induced acute liver injury by activating Nrf2 signaling pathway in mice. *Environ Toxicol.* (2018) 33:1050–60. doi: 10.1002/tox.22616

**Conflict of Interest Statement:** The authors declare that the research was conducted in the absence of any commercial or financial relationships that could be construed as a potential conflict of interest.

Copyright © 2018 Fan, Song, Wang, Li, Yang and Yu. This is an open-access article distributed under the terms of the Creative Commons Attribution License (CC BY). The use, distribution or reproduction in other forums is permitted, provided the original author(s) and the copyright owner(s) are credited and that the original publication in this journal is cited, in accordance with accepted academic practice. No use, distribution or reproduction is permitted which does not comply with these terms.

RETRACTED